Neoproterozoic and post-Caledonian exhumation and shallow faulting in NW Finnmark from K/Ar dating and p/T analysis of fault-rocks

Jean-Baptiste P. Koehl[1,2], Steffen G. Bergh[1,2], Klaus Wemmer[3]

6) Department of Geosciences, University of Tromsø, N-9037 Tromsø, Norway.
7) Research Center for Arctic Petroleum Exploration (ARCEx), University of Tromsø, N-9037 Tromsø, Norway.
8) Geoscience Centre, Georg-August-University Göttingen, Goldschmidtstraβe 3, 37077 Göttingen, Germany.

Abstract. Well-preserved fault gouge along brittle faults in Paleoproterozoic, volcano-sedimentary rocks of the Raipas Group exposed in the Alta-Kvænangen tectonic window in northern Norway yielded latest Mesoproterozoic (ca. 1050 ± 15 Ma) to mid Neoproterozoic (ca. 825-810 ± 18 Ma) K/Ar ages. Pressure-temperature estimates from microtextural and mineralogy analyses of fault-rocks indicate that brittle faulting may have initiated at depth of 5-10 km during the opening of the Asgard Sea in the latest Mesoproterozoic-early Neoproterozoic (ca. 1050-945 Ma), and continued with a phase of shallow faulting during to the opening of the Iapetus Ocean-Ægir Sea and the initial breakup of Rodinia in the mid Neoproterozoic (ca. 825-810 Ma). The predominance and preservation of synkinematic smectite and subsidiary illite in cohesive and non-cohesive fault-rocks indicate that Paleoproterozoic basement rocks of the Alta-Kvænangen tectonic window remained at shallow crustal levels (< 3.5 km) and were not reactivated since mid Neoproterozoic times. Slow exhumation rate estimates for the early-mid Neoproterozoic (ca 10-75 m per Ma) suggest a period of tectonic quiescence between the opening of the Asgard Sea and the breakup of Rodinia. In the Paleozoic, basement rocks in NW Finnmark were overthrusted by Caledonian nappes along low-angle thrust detachments during the closing of the Iapetus Ocean-Ægir Sea. K/Ar dating of non-cohesive fault-rocks and microtexture-mineralogy of cohesive fault-rock truncating Caledonian nappe units show that brittle (reverse) faulting potentially initiated along low-angle Caledonian thrusts during the latest stages of the Caledonian Orogeny in the Silurian (ca. 425 Ma) and was accompanied by epidote/chlorite-rich, stilpnomelane-bearing cataclasite (type 1) indicative of a faulting depth of 10-16 km. Caledonian thrusts were inverted (e.g. Talvik fault) and later truncated by high-angle normal faults (e.g. Langfjord-Vargsund fault) during subsequent, late Paleozoic, collapse-related widespread extension in the Late Devonian-early Carboniferous (ca. 375-325 Ma). This faulting period was accompanied by quartz- (type 2), calcite- (type 3) and laumontite-rich cataclasites (type 4), which crosscutting relationships indicate a progressive exhumation of Caledonian rocks to zeolite facies conditions (i.e. depth of 2-8 km). An ultimate period of minor faulting occurred in the late Carboniferous-mid Permian (315-265 Ma) and exhumed Caledonian rocks to shallow depth 1-3.5 km. Alternatively, late Carboniferous (?) - early/mid Permian K/Ar ages may reflect late Paleozoic

weathering of the margin. Exhumation rates estimates indicate rapid Silurian-early Carboniferous exhumation and slow exhumation in the late Carboniferous-mid Permian, supporting decreasing faulting activity from the mid-Carboniferous. NW Finnmark remained tectonically quiet in the Mesozoic-Cenozoic.

1. Introduction

Onshore and nearshore areas of Finnmark and shallow parts of the Barents shelf, such as the Finnmark Platform, are underlain by Archean-Paleoproterozoic basement rocks exposed onshore in coastal ridges (Zwaan, 1995; Bergh et al., 2010) and tectonic windows (Reitan, 1963; Roberts, 1973; Zwaan & Gautier, 1980; Gautier et al., 1987; Bergh & Torske, 1988; Jensen, 1996) of the overlying Caledonian nappe stack (Roberts, 1973; Corfu et al., 2014). These basement rocks are part of the Fennoscandian Shield onto which Caledonian nappes were overthrusted in the Silurian (Townsend, 1987; Corfu et al., 2014; Figure 1). Post-Caledonian extension started in the Devonian (Roberts et al., 2011; Davids et al., 2013; Koehl et al., 2018) with reactivation of Proterozoic and Caledonian ductile fabrics and continued through the mid Permian and, later on, through the Mesozoic and early Cenozoic when multiple brittle faults onshore and nearshore and major offshore rift basins formed prior to the opening of the NE Atlantic Ocean (Breivik et al., 1995; Gudlaugsson et al., 1998; Bergh et al., 2007; Faleide et al., 2008; Indrevær et al., 2013; Koehl et al., 2018).

Critical to the understanding of post-Caledonian extension and brittle fault evolution is the nature and timing of faulting. We have dated multiple brittle faults using K-Ar method of non-cohesive fault rocks (Lyons & Snellenburg, 1971) along several major brittle faults in NW Finnmark, along fault segments of the Trollfjorden-Komagelva Fault Zone (TKFZ; Siedlecka & Siedlecki, 1967; Siedlecki, 1980; Herrevold et al., 2009; Figure) and Langfjorden-Vargsundet fault (LVF; Zwaan & Roberts, 1978; Lippard & Roberts, 1987; Figure). The TKFZ, which crops out in northern (Koehl et al. submitted) and eastern Finnmark (Siedlecki, 1980), represents a major Neoproterozoic fault zone that was active through various episodes of (Timanian and Caledonian) transpression and subsequent extension (Herrevold et al., 2009), whereas the LVF corresponds to a large, zigzag-shaped, NE-SW trending, margin-parallel fault complex which age is yet uncertain (Zwaan & Roberts, 1978; Roberts & Lippard, 2005; Koehl et al., submitted). This fault, however, extends onto the Finnmark Platform east where it bounds a triangular-shaped, half-graben basin of presumed Carboniferous age (Figure ; Koehl et al., 2018).

The main goal of this work is to constrain the timing of brittle fault initiation (Proterozoic and/or post-Caledonian), and to discuss the reactivation and exhumation history of faults in basement rocks and Caledonian units of NW Finnmark,. We focus on margin-parallel brittle faults in basement rocks of the Alta-Kvænangen tectonic window in the Altafjorden area, for comparison with exposed fault segments of the Neoproterozoic, margin-oblique TKFZ (Figure). We also mapped and analyzed post-

Caledonian fault segments and splays of the margin-parallel LVF to compare with the age of similar, offshore, basin-bounding faults (e.g. Troms-Finnmark and Måsøy fault complexes; Figure) and associated syn-tectonic sedimentary rocks on the Finnmark Platform and in offshore basins, e.g. the Hammerfest and Nordkapp basins (Gabrielsen et al. 1990; Indrevær et al., 2013).

A second goal is to evaluate the amount of exhumation the margin underwent from the Neoproterozoic to the Caledonian Orogeny and from the collapse of the Caledonides to present times. Thus, we sampled cataclastic fault-rocks along multiple brittle faults including brittle faults that crosscut Archean-Paleoproterozoic rocks in fresh road cuts in Altafjorden, and faults like the LVF and TKFZ in Caledonian thrust nappe rocks (Figure). Then, we analyzed characteristic mineral assemblages for each cataclastic fault-rock, i.e. each faulting event recorded, which we used in conjunction with crosscutting relationships between fault-rocks to reconstruct the evolution of p/T conditions (i.e. depth) during faulting and, thus, resolve the exhumation history of the margin. We compare our results with those from analog studies in Western Troms (Davids et al., 2013; Indrevær et al., 2014; Davids et al., submitted) and Finnmark (Torgersen et al., 2014), and discuss regional implications for the tectonic evolution of the Troms-Finnmark margin during post-Caledonian extension.

2. Geological setting

2.1. Precambrian basement rocks and Caledonian nappes

The bedrock geology of NW Finnmark consists of Archean-Paleoproterozoic metavolcanic and metasedimentary rocks that occur in tectonic windows, e.g. the Alta-Kvænangen (Bøe & Gautier, 1978; Zwaan & Gautier, 1980; Gautier et al., 1987; Bergh & Torske, 1988), Altenes (Jensen, 1996) and Repparfjord-Komagfjord tectonic windows (Reitan, 1963; Pharaoh et al., 1982, 1983), overlying Caledonian nappes, e.g. Kalak Nappe Complex (Ramsey et al., 1979, 1985; Kirkland et al., 2005) and Magerøy Nappe (Andersen, 1981, 1984), and intruded by igneous rocks of the Seiland Igneous Province (Elvevold et al., 1994; Pastore et al., 2016) and Honningsvåg Igneous Complex (Corfu et al., 2006). Precambrian basement rocks are variably metamorphosed but generally show greenschist facies mineral assemblages in the study area (Bøe & Gautier, 1978; Zwaan & Gautier, 1980; Bergh & Torske, 1988).

The Caledonian Kalak Nappe Complex is thought to represent a Laurentia-derived unit that was thrusted over Precambrian basement rocks of Baltica during the Caledonian Orogeny (Kirkland et al., 2008). Metasedimentary rocks of the Kalak Nappe Complex were metamorphosed to amphibolitic facies conditions and are composed of metapsammites, schists and paragneisses crosscut by low-angle thrusts and shear zones (Ramsey et al., 1979; 1985). The Kalak Nappe Complex is intruded by mafic and ultramafic rocks of the Seiland Igneous Province (Elvevold et al., 1994) that form two deep roots below the island of Seiland and Sørøya (Pastore et al., 2016). The structurally overlying Magerøy Nappe is made of tightly folded, greenschist facies, metasedimentary rocks that are separated from the Kalak

Nappe Complex by a low-angle thrust onshore Magerøya (Andersen, 1981, 1984). This nappe unit was intruded by mafic rocks of the Honningsvåg Igneous Complex during the Caledonian Orogeny (Corfu et al., 2006).

2.2. Brittle faulting and previous age dating in North Norway

2.2.1.Brittle faults trends

Precambrian basement rocks and Caledonian nappes in coastal areas of northern Norway are truncated by several major brittle faults and fracture sets, striking NNE-SSW, ENE-WSW and WNW-ESE (Bergh et al. 2007; Eig & Bergh 2011; Indrevær et al. 2013; Koehl et al. submitted) and of presumed post-Caledonian age. The timing of formation of these faults is uncertain and yet unresolved, but most are thought to be post-Caledonian (Davids et al., 2013, submitted), although Precambrian ages cannot be excluded (Torgersen et al., 2014; Koehl et al., submitted). The three fault sets commonly form two major fault systems. On the one hand, NNE-SSW and ENE-WSW faults often interact to produce zigzag-shaped fault complexes. An example in NW Finnmark is the LVF, which is made up of alternating ENE-WSW and NNE-SSW trending fault segments (Zwaan & Roberts, 1978; Lippard & Roberts, 1987; Koehl et al. submitted) and resembles the offshore, basin-bounding, zigzag-shaped Troms-Finnmark Fault Complex in map-view (Figure ; Indrevær et al. 2013). This resemblance is verified by offshore prolongation of the LVF into shallow Carboniferous half-graben on the Finnmark Platform east (Koehl et al., 2018). On the other hand, WNW-ESE striking faults are usually observed as swarms of high-frequency, (sub-) parallel fractures. A key example is the TKFZ, a major Neoproterozoic fault zone that extends from the Varanger Peninsula in the east and crops out onshore the island of Magerøya in the west (Figure). This fault complex is made up with multiple segments of sub-parallel, WNW-ESE trending brittle faults that die out just west of Magerøya (Koehl et al. submitted). Several of these fault segments were intruded by highly magnetic dolerite dykes during an early Carboniferous extensional event (Roberts et al. 1991; Lippard & Prestvik 1997; Nasuti et al. 2015), when the TKFZ acted as a strike-slip transfer fault and segmented onshore-nearshore areas of NW Finnmark from the offshore Finnmark Platform east during late/post-Caledonian extension (Koehl et al., 2018, submitted).

2.2.2.Dating of brittle faults in North Norway

Previous K-Ar dating of synkinematic illite/muscovite in fault gouge in NW Finnmark show that brittle faults in the Repparfjord-Komagfjord tectonic window, like the Kvenklubben fault, formed in Precambrian times and were reactivated as Caledonian thrust and, later on, as normal faults during late/post-orogenic extension and subsequent rifting (Torgersen et al. 2014). Non-cohesive fault-rocks sampled by Torgersen et al. (2014) showed enrichment in authigenic smectite and chlorite clay minerals and a rather low content of illite/muscovite.

Farther southwest along the margin, in Western Troms, similar coastal brittle faults display cohesive cataclastic fault-rocks with epidote, chlorite and pumpellyite (Indrevær et al. 2014), and these faults are juxtaposed with amphibolite facies Precambrian rocks of the West Troms Basement Complex (Zwaan 1995; Bergh et al. 2010). These faults are interpreted to have formed during late Paleozoic extension at depth > 10 km and to have been exhumed to shallower crustal level < 8.5 km, as shown by the widespread occurrence of pumpellyite mineral in fault-rocks. These faults yielded late Paleozoic K/Ar ages and are possibly associated with post-Caledonian extension in the Devonian-Carboniferous (Davids et al. 2013).

3. Methods

3.1. Structural field data

In summer 2015, we acquired extensive structural field data along brittle faults in NW Finnmark, which we compiled, interpreted and discussed in earlier contributions (Bergø, 2016; Lea, 2016; Koehl et al., submitted). Among the numerous brittle faults cropping out in NW Finnmark, we selected ten based on their proximity to major faults (e.g. LVF, TKFZ), location relative to major faults (footwall/hanging-wall) and according to their strike (parallel to dominant fault trends in Finnmark), which we briefly describe from a structural perspective at outcrop scale. Fault geometries and kinematic indicators will be used in conjunction with cohesive and non-cohesive fault-rock composition and with the result of K/Ar dating of fault gouge to propose an evolutionary model for the tectonic evolution and exhumation history of the SW Barents Sea margin and NW Finnmark.

3.2. Microscopic analysis of onshore cohesive fault-rock

We collected cohesive fault-rock samples along numerous brittle faults we encountered in NW Finnmark (including the ten dated faults), and we used them to investigate kinematic indicators along the selected brittle faults at microscale. We also studied mineral assemblages included in brittle fault-rocks in order to constrain metamorphic facies (p/T) conditions during faulting, therefore adding to the understanding of the exhumation and uplift history of the SW Barents Sea margin. When needed, thin sections were analyzed through an optical microscope and a Scanning Electron Microscope (SEM) at the University of Tromsø to obtain more detailed information about mineral composition.

3.3. K/Ar dating and mineralogical analysis of fault gouge

We sampled non-cohesive fault-rock along brittle faults in NW Finnmark and attempted to date authigenic (i.e. synkinematic) illite clay mineral formed during faulting events (e.g. Vrolijk & van der

Pluijm, 1999; Davids et al., 2013; Torgersen et al., 2014; Ksienzyk et al., 2016), which platy crystal shape differs from their irregular detrital counter-part (e.g. Davids et al., 2013; Torgersen et al., 2014). The ten dated samples of non-cohesive fault-rock are referred to as sample 1-10 in the text and figures. K/Ar dating of fault gouge was carried out in the K/Ar laboratory facility at the University of Göttingen, Germany. Three grainsize fractions were analyzed for each sample: "2-6 µm", "< 2 µm" and "< 0.2 µm". Clay-rich fault gouge samples were resolved in water and wet-sieved using a 63 µm sieve. The fraction < 63µm was used to extract the clay fractions < 2µm by settling in Atterberg cylinders. The fractions < 0.2µm have been separated using an ultra-centrifuge. All these fine fractions were examined (XRD) for mineralogical composition and determination of the illite crystallinity using a PHILIPS PW 1800 diffractometer

Illite crystallinity, the peak width at half height of the 10-Å peak, was determined using a computer program developed at the University of Göttingen. Digital measurement of illite crystallinity was carried out by step scan (301 points, 7-10° 2Θ, scan step 0.010° 2Θ, integration time 4 s, receiving slit 0.1mm, automatic divergence slit). Illite crystallinity determinations have shown to be a sensitive indicator for the degree of very low grade metamorphism in clastic sediments. Reviews of the preparation techniques and the interpretation have been given for example by Kisch (1991) and Krumm (1992). All samples have been investigated in duplicates (A and B). The measurements were carried out in the „air dry" and the „ethylene glycol saturated" status in order to detect expandable layers of smectite type minerals. Smectite classification (Reichweite) has been determined following Moore & Reynolds (1997). Illite crystallinity is expressed as Kübler Index in (KI, Δ°2Θ), the limits for diagenesis/anchizone (ca. 200°C) and anchizone/epizone (300°C) are 0.420° and 0.250° Δ°2Θ (Kübler 1967, 1968, 1984), respectively.

The argon isotopic composition was measured in a pyrex glass extraction and purification line coupled to a Thermo Scientific ARGUS VI ™ noble gas mass spectrometer operating in static mode. The amount of radiogenic ^{40}Ar was determined by isotope dilution method using a highly enriched ^{38}Ar spike from Schumacher, Bern (Schumacher, 1975). The spike is calibrated against the biotite standard HD-B1 (Fuhrmann et al., 1987). The age calculations are based on the constants recommended by the IUGS quoted in Steiger & Jäger (1977). Potassium was determined in duplicate by flame photometry using a BWB-XP flame photometer ™. The samples were dissolved in a mixture of HF and HNO_3 according to the technique of Heinrichs & Herrmann (1990). The analytical error for the K/Ar age calculations is given on a 95% confidence level (2σ). Details of argon and potassium analyses for the laboratory in Göttingen are given in Wemmer (1991).

Temperature constraints from illite-smectite clay minerals

Since the dominant synkinematic clay mineral in the analyzed fault-rocks are smectite and subsidiary interlayered illite-smectite clay, we use the smectite-illite clay mineral reaction to infer

maximum/minimum temperature estimates for faulting events in NW Finnmark (Eberl et al. 1993; Huang et al. 1993; Morley et al. 2018). Synkinematic illite often grows due to illitisation of smectite and, alternatively, due to dissolution-precipitation of existing clay minerals of the bedrock (Vrolijk & van der Pluijm, 1999). Illitisation along fault surfaces is enhanced by temperature increase, e.g. related to frictional heating, hydrothermal processes or burial, grain comminution, strain, changes in fluid composition and fluid/rock ration (Vrolijk & van der Pluijm, 1999). Illitisation of smectite is commonly thought to begin at a temperature range of 40-70°C (Jennings & Thompson, 1986; Harvey & Browne, 2000; Ksienzyk et al., 2016).

Interpretation of inclined age spectra

K/Ar dating requires targeted minerals to behave as "closed systems" with no loss of argon or potassium (Lyons & Snellenburg, 1971). Mineral closure temperature varies with grainsize and is lower for finer grains. For example, aggregates of fine grains may accidentally be incorporated and dated as part of coarser fractions of fault gouge, thus leading coarse fractions to yield younger ages than finer fractions (Hamilton et al., 1989; Heizler & Harrison, 1991). More specifically along shallow faults, illite grains < 2 µm crystallize below the closure temperature of the K-Ar system (> 250°C; Velde, 1965) and, thus, provide with robust, synkinematic crystallization ages rather than less accurate, generally younger cooling ages obtained along deeper faults (Hunziker et al., 1986; Ksienzyk et al., 2016). Further, contrarily to metamorphism-related heating, the short heating time associated with hydrothermal events or frictional heating along brittle faults are unlikely to reset illite ages, which would require longer exposure to temperature > 250°C (Torgersen et al., 2014), thus suggesting that K/Ar ages on illite along shallow faults provide reasonable estimates of the age of faulting.

Mixing of host-rock inherited minerals, e.g. detrital illite-muscovite, with authigenic illite may influence K/Ar ages and cause age dispersion in faults, notably in the coarser fractions dated (Hower et al., 1963; Vrolijk & van der Pluijm, 1999). However, inherited illite-muscovite may be distinguished from authigenic clay minerals as they display more irregular shapes than their generally platy authigenic counter-parts (e.g. Torgersen et al., 2014). In addition, faulting may even isotopically reset fine-grained, hostrock illite-muscovite, thus yielding ages bearing no influence of inherited, older minerals (Vrolijk & van der Pluijm, 1999). In addition, fault-inherited illite may also affect K/Ar ages, which is especially verified along repeatedly active, progressively exhumed faults because high-temperature illite may survive low-temperature reactivation of the faults (Davids et al., 2013; Viola et al., 2013). Another mineral that may have a significant impact on K/Ar ages is host rock-inherited K-feldspar. Most importantly, K-feldspar has a significantly lower closure temperature (350-150°C) than illite clay mineral (> 250°C), hence yielding younger ages than the actual age of faulting, particularly for finer fractions in fault gouges (Lovera et al., 1989). Hornblende may also affect K/Ar dating of illite (Torgersen et al., 2015) but was not encountered in any fault-rock samples in NW Finnmark and its effect are therefore not considered here.

4. Results

We sampled brittle fault rocks for K-Ar dating and microtextural analysis from several dominant fault systems and fault trends in NW Finnmark (Figure ; Koehl et al., submitted). The sampling sites include (i) faults in Paleoproterozoic rocks of the Raipas Group (Zwaan & Gautier, 1980) in Altafjorden (samples 3 & 4), (ii) faults in the Caledonian Kalak Nappe Complex along segments and splay-faults of the LVF (samples 1, 2, 5, 6 & 7), and (iii) faults in rocks of the Kalak Nappe Complex and Magerøy Nappe (sample 8, 9 & 10) adjacent to segments of the TKFZ (Figure). For the sampled faults, we first describe trends, field relations and kinematics of the faults. Second, we describe the mineral assemblages and microstructures of sampled cohesive fault-rocks in order to infer deformation mechanisms and estimate the p-T conditions during faulting and exhumation. Third, we present the K-Ar data and mineralogical results obtained on fault gouge.

4.1. Field relations of sampled brittle faults in NW Finnmark

4.1.1.Brittle faults in Paleoproterozoic basement rocks (samples 3 & 4)

Samples 3 and 4 (Figure 2a & b) are from the Altafjorden fault 1 and 2, NW-dipping brittle faults in new, fresh road-cuts along the western shore of Altafjorden, truncating meta-arkoses of the Paleoproterozoic Raipas Group (Skoadduvarri Sandstone) of the Alta-Kvænangen tectonic window (Zwaan & Gautier, 1980; Bergh & Torske, 1986, 1988). The two sampled faults are located a few tens of meters away from each other, display m-thick fault-cores mostly composed of grey-colored clay particles in non-cohesive fault gouge and partly cohesive cataclasites (Figure 2a & b). The Altafjorden fault core also show multiple slip surfaces cemented by cm-thick quartz grains (Figure 2a). Slickenside lineations on fault surfaces indicate normal dip-slip movement. A mafic band is bent into (drag folded) the fault core facilitating normal down-to-the NW sense of shear (Figure 2a). The absence of this mafic bed in the footwall of the Altafjorden fault suggests that the fault accommodated vertical displacement > 5-6 m.

4.1.2.Brittle faults along the LVF (samples 1, 2, 5, 6 & 7)

We sampled fault-rocks along several segments/splay-faults of the LVF (Torgersen et al., 2014; Koehl et al., submitted). This regional fault complex can be traced from Sørkjosen in the south (cf. location of samples 1 & 2 in Figure) to the Porsanger Peninsula in the north (Figure) and defines a zigzag-shaped pattern of alternating, NNE-SSW to ENE-WSW trending fault segments that dominantly dip WNW and NNW, respectively (Koehl et al., submitted). Samples 1 and 2 are taken from two minor NW-dipping fault splays (Figure 2c & d) in the footwall of the Sørkjosen fault, a major fault-segment of the LVF (Figure ; Koehl et al., submitted). The faults crosscut granodioritic gneisses of the Kalak

Nappe Complex and display thin, 10-40 cm-thick fault-cores with lenses of dark clayish gouge material (Figure 2c & d). The northern of these faults accommodates ca. 5-8 m top-to-the-NW, normal displacement of a 20-30 cm-thick layer of mafic amphibolite (Figure 2c), while the southern fault offsets the same mafic layer by ca. 2 m top-to-the-NW (Figure 2d). Slickenside lineations along these two faults support normal dip-slip sense of shear (Figure 2c & d).

Along strike northeastward, we sampled another subsidiary fault linked to the LVF along the western shore of Altafjorden, the Talvik fault (sample 5; Figure), a low-angle, N-dipping fault that crosscuts arkosic meta-psammites of the Kalak Nappe Complex (Figure 2e). The Talvik fault shows evidence of both brittle and ductile faulting in a ca. one meter-thick fault-core made of semi-ductile, mylonitic fault-rock, overprinted by calcite- and quartz-bearing cataclasite, as well as thin layers of non-cohesive fault gouge along distinct fault surfaces (Figure 2e). Field observations of quartz-sigma clasts and S-C fabrics in the mylonites reveal top-to-the-south thrusting, whereas slickengrooves and asperities are present along distinct brittle fault surfaces, implying top-to-the-N motion along the Talvik fault (Figure 2e). Brittle offset of ductile quartz sigma-clasts confirms that brittle fabrics are younger than ductile fabrics.

Sample 6 was taken along a high-angle, NNE-SSW trending and WNW-dipping brittle fault that crops out along the eastern shore of Altafjorden (cf. Figure and Figure 2f). This fault defines the southeastern boundary of a graben structure in garnet-rich meta-psammite of the Kalak Nappe Complex and is characterized by a ca. one meter-thick fault-core made of non-cohesive clayish fault gouge and adjacent epidote-rich cataclasite (Figure 2f). Slickenside lineations indicate down-to-the-WNW, dip-slip normal movement, which is consistent with normal dip-slip offsets of boudinaged mafic dykes across nearby NNE-SSW trending faults (Figure 2f).

The final fault-rock sample along LVF segments and splays (sample 7; Figure) is from the steep, NNE-SSW trending, SE-dipping Snøfjorden-Slatten fault on the Porsanger Peninsula (cf. Figure and Figure 2g; Passe, 1978; Townsend, 1987b), which represents a major, antithetic fault segment/splay of the LVF (Koehl et al., submitted). This fault crosscuts felsic metasedimentary rocks and micaschists of the Kalak Nappe Complex and displays a several meter-wide fault-core that is made of non-cohesive iron- and quartz-rich fault gouge, including a few lenses of cohesive fault-rock (Figure 2g). Slickensided fault surfaces reveal down-to-the-SE, normal dip-slip movement, probably a few meters to a few tens of meters due to the presence of the same host rock on both sides of the fault (Figure 2g).

4.1.3.Brittle faults adjacent to the TKFZ (samples 8, 9 & 10)

Subvertical, WNW-ESE trending brittle faults and fracture systems are widespread near and within Magerøy Nappe units on the Porsanger Peninsula and the island of Magerøya (Figure ; cf. Koehl et al. submitted). Sample 8 is from fault gouge found along an anomalously low-angle, WNW-ESE striking, NNE-dipping fault on the Porsanger Peninsula (Figure and Figure 2h). The fault crosscuts garnet-mica gneisses of the Kalak Nappe Complex, adjacent to a lens of preserved Magerøya Nappe

unit on the Porsanger Peninsula (Kirkland et al., 2007). This fault comprises thin, dm-scale lenses of dark clay particles along the fault-core and damage zone with splaying fault geometries (Figure 2h). Oblique normal-sinistral movement is inferred from slickenside lineations (Figure 2h), and the amount of displacement probably does not exceed a few tens of meters because garnet-bearing gneisses occur on both sides of the fault.

Farther north, sample 9 corresponds to a steep, WNW-ESE to E-W trending, S-dipping fault (Figure and Figure 2i) in a new quarry within a suite of weakly foliated gabbroic rocks of the Honningsvåg Igneous Complex (Corfu et al., 2006). The sampled fault-core includes two thin, 5-10 cm-thick layers of light-colored, non-cohesive clay particles (Figure 2i).

The last fault we sampled for K/Ar dating (sample 10) was taken along a steep, WNW-ESE striking, NNE-dipping brittle fault in the western part of Magerøya (cf. Figure and Figure 2j). This fault is part of a high-frequency, WNW-ESE trending lineament and brittle fault system that corresponds to fault segments of the TKFZ, which pervasively truncate metasedimentary rocks of the Kalak Nappe Complex in western Magerøya (Koehl et al., submitted) and displays a ca. 0.5 m-thick fault-core made up with light-colored clay particles (Figure 2j).

4.2. Mineralogy and microtextural analysis of cohesive fault-rock

4.2.1.Cohesive fault-rocks within the Alta-Kvænangen tectonic window

In order to describe and analyze cohesive brittle fault-rock characters and mineralogical and textural changes during cataclasis, the host rock characters are used as frame. Cohesive fault-rock was found along most exposed brittle faults crosscutting Precambrian volcano-sedimentary rocks of the Alta-Kvænangen tectonic window (Figure 2a & b). The host rocks are fairly undeformed but underwent low-grade (greenschist facies) metamorphic conditions during the Svecofennian Orogeny , and developed a weak, bed-parallel foliation (Bøe & Gautier, 1978; Zwaan & Gautier, 1980; Bergh & Torske, 1988). This foliation comprises partly recrystallized, sigma-shaped grains of quartz and feldspar locally incorporated into an S-C foliation made of elongated crystals of white mica (Figure 3a).

Brittle faults analyzed in the present study crosscut both meta-sandstones and metamorphosed carbonate-rich host-rocks, and include three types of cataclasites and mineral precipitations. The first type shows a matrix of finely crushed clasts of quartz (Figure 3b). The second type is made of a partly healed, calcite-cemented cataclasite, which crystals display both type II and IV twinning (Lerman 1999; Figure 3c). The third type includes cataclasite with abundant brownish to reddish matrix of very fine-grained clay- (smectite and subsidiary illite) and iron-rich minerals associated with iron-bearing precipitations, often truncating veins of recrystallized quartz and quartz-rich cataclasite (Figure 3b). Iron-bearing precipitations often appear to localize along fractures developed parallel to pre-existing, white-mica, S-C-C’ foliation (Figure 3b). Relative timing of quartz-, calcite- and clay-rich cataclasite could not be directly resolved from crosscutting relationships.

4.2.2.Cohesive fault-rocks within Caledonian nappes

Metamorphic Caledonian host rocks consist of a variety of granodioritic gneisses, metasandstones, metapelites, amphibolites/metavolcanics, gabbros and micaschists. When truncated by brittle faults, most rocks are altered and/or display retrograde mineral assemblages. Notably, in mafic/granodioritic host rocks, biotite is systematically retrograded into chlorite in the vicinity of brittle faults (Figure 3d), host rocks are generally enriched in epidote at the expense of amphibole, and garnet porphyroblasts are highly fractured (Figure 3e). Brittle faults crosscutting Caledonian rocks comprise up to 1-2 m wide lenses of fractured host rocks showing preserved ductile fabrics, such as widespread muscovite-biotite and S-C-C' foliation with feldspar sigma-clasts partly recrystallized into quartz (e.g. along the Sørkjosen and Snøfjorden-Slatten faults; Figure 3d & f). Typically, S, C and C' foliation surfaces are partly replaced by cataclastic fault-rocks and, thus, may have localized subsequent brittle faulting (Figure 3g), as observed along the brittle-ductile Talvik fault (Figure 2e).

We identified five texturally different types of cataclasites crosscutting each other in a systematic order. The first type of cataclasite (type 1) is made of fine-grained, rounded to sub-rounded clasts of epidote and chlorite (Figure 3e & h), often reworked into large, angular clasts incorporated into subsequent cement or cataclastic matrix (Figure 3e & i). Epidote-chlorite fracture precipitations sometimes appear undeformed (Figure 3j). Occasionally, epidote-chlorite bearing veins comprise rounded clasts of a brownish mineral showing moderate to strong relief (Figure 3h). EDS analysis reveals that this mineral is enriched in calcium, iron, silica, aluminium, magnesium and oxygen (Figure 3k), and, thus, may correspond to stilpnomelane (Eggleton, 1972).

The second type of cataclasite (type 2) is composed of very fine-grained, rounded to sub-rounded clasts of quartz (Figure 3h). This type of cataclasite is often observed adjacent to host rock clasts (Figure 3e), regularly incorporates angular clasts of epidote-rich cataclasite (Figure 3e & h), and occurs in conjunction with veins of recrystallized quartz (Figure 3h).

The third type of cataclasite (type 3) is widespread along fault segments and splay-faults of the LVF (e.g. Sørkjosen, Straumfjordbotn, Langfjorden, Øksfjorden, Altafjorden 1 & 2, and Talvik faults) and is characterized by poorly sorted, angular clasts of calcite (Figure 3l) often associated with abundant, locally undeformed, calcite cement, showing type I and type II twinning (Figure 3i; Lerman 1999). Calcite crystals consistently crosscut veins of recrystallized quartz, and epidote- and quartz-rich cataclasites (Figure 3e).

The fourth type of cataclasite (type 4) consists of abundant, new-grown, mildly cataclased, prismatic/columnar mineral grains with acute edges and steep-oblique terminations showing low relief, low refraction index and three sets of cleavage (Figure 3e & m). We interpret this mineral as laumontite, i.e. a high-temperature zeolite mineral (Dill et al., 2007; Triana et al., 2012). In the study area, laumontite crystals commonly grew with their long-crystallographic axis perpendicular to brittle fractures (Figure

3m) and consistently crosscut epidote- and quartz-rich cataclasites and epidote-chlorite and calcite-filled veins (cf. Figure 3e).

The fifth type of cataclasite (type 5) shows enrichment in very fine-grained, iron-oxide bearing mineral precipitations and an even more fine-grained, microscopic matrix of brownish and greyish clay minerals (Figure 3e, h, l & n). These cataclastes truncate and often incorporate clasts of epidote-chlorite, quartz- and calcite- rich cataclasite and associated mineral veins (cf. Figure 3e, l & n).

4.3. Fault gouge mineralogy and K/Ar ages

4.3.1.Mineralogy

XRF analyses of various grainsize fractions of the sampled fault gouges in NW Finnmark consistently show (1) high smectite content often associated with chlorite (mixed-layer chlorite-smectite), e.g. samples 1, 2, 6 & 8 (Figure), (2) a relatively low content in illite and (3) variable amount of residual quartz (Table 1 &Appendix 1). The only exception is sample 8 from the Porsanger Peninsula (cf. Figure 2h), which contains higher amounts of illite and quartz together with smectite, chlorite and kaolinite clay minerals (Table 1 & Appendix 1). The analysis of the diffraction spectrum for all three grainsize fractions indicates that fault gouge from western Magerøya (sample 10) is made of almost pure smectite (Figure 2j, Table 1 and Appendix 1). Traces of K-feldspar, indicated by minor peaks at 27.3-27.4 on inclined spectra (Table 1 & Appendix 1), were observed in all three grainsize fractions of fault gouge samples 1 & 2 in Sørkjosen (Figure , Figure 2c & d, Table 1 & Appendix 1), in the coarse (2-6 µm) fraction of sample 6 from the eastern shore of Altafjorden (Figure , Figure 2f, Table 1 & Appendix 1), in the coarse and intermediate fractions of sample 7 from the Snøfjorden-Slatten fault on the Porsanger Peninsula (Figure , Figure 2g, Table 1 & Appendix 1), and in sample 10 along a WNW-ESE trending fault in western Magerøya (Figure , Figure 2j, Table 1 & Appendix 1). Sample 9 from the Honningsvåg Igneous Complex on Magerøya (Figure 2i) shows very low potassium content (cf. Table 2), which resulted in high 2σ errors associated with the K/Ar ages obtained for all three fractions (cf. Table 2). We also noticed the presence of possible laumontite and/or stilbite in this sample (Table 1 & Appendix 1; Triana et al., 2012).

4.3.2.K/Ar dating results

Precambrian ages

All three dated fractions of sample 3 and 4 (Figure & Figure 2a & b) yielded Precambrian ages (Table 2, Figure 4 & Figure 5). For sample 3, the coarse fraction yielded a late Mesoproterozoic age (1050.7 ± 12.2 Ma; cf. Figure 4 & Figure 5). The intermediate and finest fractions of this sample both yielded early Cryogenian (Neoproterozoic) ages, 806.4 ± 10.7 and 824.7 ± 12.7 Ma respectively (Table 2 & Figure 4 & Figure 5). The intermediate fraction yielded a slightly younger age in tendency compared

to the finest fraction, taking the errors into account, both ages do not differ significantly. Nevertheless, these K/Ar ages from well-preserved, non-cohesive fault gouges suggest that the Altafjorden fault 1 (Figure 2a) formed in late Mesoproterozoic times and was reactivated at least once in the Neoproterozoic (early Cryogenian). Younger, post-Caledonian reactivation seems unlikely, as the sensitivity of the K/Ar geochronometer would certainly have recorded subsequent reactivation by yielding younger ages.

Similar Precambrian K-Ar ages were obtained for the three fractions of sample 4 from the Altafjorden fault 2 (Figure , Figure 2b, Figure 4 & Figure 5). Here, the coarse-grained fraction yielded a late Mesoproterozoic age of 1054.2 ± 14.7 Ma, the intermediate fraction a Tonian (early Neoproterozoic) age of 943.8 ± 17.3 Ma, and the finest fraction a Cryogenian (mid Neoproterozoic) age of 811.3 ± 17.8 Ma (Table 2, Figure 4 & Figure 5). Considering the proximity of the Altafjorden faults 1 and 2 (samples 3 & 4; Figure) and the comparable ages obtained for these faults, we consider the K/Ar ages to be reliable and likely reflecting protracted Mesoproterozoic-Neoproterozoic tectonic events. These results further suggest that the Altafjorden faults 1 and 2 were not reactivated in the Phanerozoic, as further reactivation would necessarily have been recorded and resulted in younger ages.

Late Paleozoic ages

Most of the dated fault gouges from segments of the LVF in the Kalak Nappe Complex, as well as those along the TKFZ on the Porsanger Peninsula and Magerøya yielded late Paleozoic ages (Table 2, Figure 4 & Figure 6). The coarse fraction of the Talvik fault (sample 5; Figure & Figure 2e) yielded a Silurian age of 427.3 ± 8.4 Ma, the intermediate fraction a Tournaisian (early Carboniferous) age of 353.7 ± 4.1 Ma and the finest fraction an early Permian age of 282.1 ± 6.3 Ma (Figure 4 & Figure 6). These ages may indicate brittle faulting at the end of the Caledonian Orogeny and reactivation during post-Caledonian extension in the early Carboniferous-mid Permian, (see discussion).

The intermediate and fine-grained fractions of sample 6 along the eastern shore of Altafjorden (Figure & Figure 2f) yielded earliest Permian and latest Carboniferous ages respectively (292.6 ± 4.0 Ma; 298.5 ± 5.0 Ma), while the coarse-grained fraction yielded a Jurassic age of 208.5 ± 3.1 Ma (Table 2, Figure 4 & Figure 6). A possible explanation for this discrepancy is that the coarse fraction of sample 6 partly consists of aggregates of smaller grains reflecting a much younger faulting event (Hamilton et al., 1989; Heizler & Harrison, 1991). However, XRF analysis of the sample suggests that the anomalous, younger age obtained for the coarse fraction may be the product of excess potassium due to the presence of K-feldspar in the sample (cf. Table 1 & Appendix 1; Lovera et al., 1989).

The sample taken along the low-angle, WNW-ESE trending fault on the Porsanger Peninsula (sample 8; Figure & Figure 2h) yielded similar latest Carboniferous-earliest Permian ages all included within a 5 Ma time span of 302.3 ± 6.5 Ma, 297.6 ± 7.7 Ma and 296.6 ± 3.8 Ma (cf. Table 2, Figure 4 & Figure 6). This suggests that the fault was not reactivated after the earliest Permian, as the finest fraction would have recorded a younger faulting event and, thus, yielded a younger age. It is, however, possible that the fault accommodated earlier faulting events.

Fault gouge sampled along a WNW-ESE trending fault segment of the TKFZ near Gjesvær in western Magerøya (sample 10; Figure & Figure 2j) yielded late Carboniferous (312.5 ± 8.7 Ma), early Permian (284.0 ± 6.2 Ma) and mid Permian (270.8 ± 6.0 Ma) ages, respectively, for the coarse, intermediate and finest fractions, suggesting the fault experienced multiple extensional faulting events from the late Carboniferous to mid-Permian (Table 2, Figure 4 & Figure 6).

Fault gouge sample 9 from an E-W to WNW-ESE trending fault within the Honningsvåg Igneous Complex in the Magerøy Nappe (Figure & Figure 2i), contains very low amounts of potassium (Table 2). This, together with a high contamination of atmospheric argon, resulted in high errors for all three dated fractions. Considering the high 2σ error percentage associated to the K/Ar ages obtained for this sample, the coarse fraction may cover a time span of faulting from the mid-Carboniferous (early Serpukhovian) to the Late Pennsylvanian (Gzhelian), 315.6 ± 13.6 Ma (Table 2, Figure 4 & Figure 6). The finest fraction exhibits an even higher 2σ error percentage, and the age window included within 2σ interval spans from the early Permian to the Middle Triassic (Table 2, Figure 4 & Figure 6). The intermediate fraction yielded a younger age (234.7 ± 18.0 Ma) than the finest fraction (265.2 ± 23.6 Ma), which is considered to be erroneous. Brittle faulting along this fault most likely initiated in the mid-Carboniferous and the fault was later reactivated in the Permian.

Mesozoic ages

Mesozoic K-Ar ages were obtained for the Snøfjorden-Slatten fault on the Porsanger Peninsula (sample 7; Figure & Figure 2g), which yielded Middle (238.0 ± 5.4 Ma) - Late Triassic (227.4 ± 5.3 Ma) to Hettangian (earliest Jurassic; 200.4 ± 6.0 Ma) ages (Table 2, Figure 4 & Figure 6). This sample, however, contains minor K-feldspar in the coarse and intermediate grainsize fractions, which may have induced an excess of potassium, hence yielding younger ages than the age of faulting (Lovera et al., 1989). Nonetheless, the Hettangian age obtained for the finest fraction seems reasonable and most likely reflects an actual faulting event.

Fault gouge of the coarse, intermediate and fine grainsize fractions of sample 1 taken near the Sørkjosen fault segment of the LVF (Figure & Figure 2c) yielded a latest Triassic (Rhaetian) age of 206.8 ± 2.6 Ma, and Late Jurassic (late Kimmeridgian) ages of 153.2 ± 3.7 Ma and 153.4 ± 1.9 Ma, respectively (Table 2, Figure 4 & Figure 6), possibly suggesting that this fault splay of the LVF formed in the latest Triassic and was reactivated in the Late Jurassic. Similar K-Ar ages were obtained for another splay fault of the LVF in Sørkjosen (sample 2; Figure & Figure 2d), i.e. Olenekian 247.6 ± 3.7 Ma and 249.4 ± 3.3 Ma (Early Triassic) ages for the coarse and intermediate fractions and a latest Mid Jurassic age of 164.4 ± 4.5 Ma for the finest fraction (Table 2, Figure 4 & Figure 6). Similarly to the other fault in Sørkjosen (sample 1), it is possible that the gouge in sample 2 formed in the Early Triassic and was reactivated during the Mid Jurassic (Table 2, Figure 4 & Figure 6). However, minor K-feldspar content observed in the diffraction spectrums of all three grainsize fractions of both of these faults

suggest the K-Ar ages probably post-date the actual faulting, but it is uncertain by how much time (Table 1 & Appendix 1).

5. Discussion

We combine mineral assemblages in cohesive and non-cohesive fault-rocks to reconstruct the faulting and burial-exhumation history of the NW Finnmark margin, using an average geothermal gradient of 30°C/km, and utilizing the K-Ar dating results of authigenic illites in non-cohesive fault-rocks to constrain the timing of faulting. The discussion starts with the estimated p-T conditions and the Mesoproterozoic-Neoproterozoic K/Ar ages obtained for the Altafjorden faults 1 & 2, and proceeds with mid-late Paleozoic, and, finally, Mesozoic exhumation (p/T) and faulting data obtained from the LVF and TKFZ as basis for comparison with p-T constraints and K/Ar faulting ages from in Western Troms.

5.1. Mesoproterozoic-Neoproterozoic faulting and exhumation history

5.1.1.Evolution of temperature conditions in Precambrian rocks

Microtextural and mineralogical analysis of cohesive fault-rocks along the Altafjorden faults 1 & 2 (Figure 2a & b) show that brittle faulting initiated with the formation of quartz- and calcite-rich cataclasites (Figure 3b & c). On the one hand, quartz-rich cataclasite derived from a foliated, meta-psammitic host rock with quartz/feldspar sigma-clasts (Figure 2a & b and Figure 3a). On the other hand, calcite-cemented cataclasite often incorporate crystals with type II and IV twinning, which indicate that these crystals were subjected to temperature ranges of 150-300°C (i.e. 5-10 km depth) and > 250°C (depth > 8 km) respectively (Figure 3c; Lerman, 1999).

Quartz-rich and calcite-cemented cataclasites are truncated and occasionally incorporated into subsequent iron/clay-rich cataclasites (Figure 3b & c). XRF analyses of non-cohesive fault-rocks sampled along the Altafjorden faults 1 & 2 (samples 3 & 4) show a dominance of smectite (Table 1 & Appendix 1), which suggests that the dominant clay mineral in related iron/clay-rich cohesive fault-rock shown in Figure 3b is smectite. Considering such a predominance of authigenic smectite in both non-cohesive and cohesive, iron/clay-rich fault-rocks (Figure 3b, Table 1 & Appendix 1), and assuming a complete diagenetic transformation of smectite into illite at ca. 105°C (cf. Morley et al., 2018) and a complete absence of authigenic illite at temperature < 35°C (Eberl et al., 1993), we propose that clay-rich fault-rocks along brittle faults in the Alta-Kvænangen tectonic window formed at temperature conditions comprised between 35-105°C (i.e. 1-3.5 km depth). Although crosscutting relationships of calcite-rich cataclasite with quartz- and iron/clay-rich fault-rocks are unknown, the irreversibility of the diagenetic transformation of smectite into illite (Eberl et al., 1993) suggests that calcite-cemented cataclasite, which formed at 5-10 km depth, is older than the iron/clay-rich (cohesive and non-cohesive) fault-rocks, which formed at shallow depth 1-3.5 km. Hence, we argue that Precambrian basement rocks

in Altafjorden experienced at least three brittle faulting events, starting with quartz-rich cataclasite (Figure 3b) and/or calcite-cemented cataclasite formed at a depth of 5-10 km (Lerman, 1999; Figure 3c). Then, basement rocks were exhumed to shallow crustal level < 3.5 km (Morley et al., 2018) when the final, iron- and smectite-rich faulting event occurred (Figure 3b).

5.1.2.Timing of faulting and exhumation of Precambrian rocks

The latest Mesoproterozoic (ca. 1050 Ma) – early Neoproterozoic ages (ca. 945 Ma) obtained for the coarse fraction of sample 3 and the coarse and intermediate fractions of samples 4 (Table 2, Figure 4 & Figure 5), and the slickenside lineations and drag-folded foliation indicating down-to-the-NNW normal motions along both faults (Figure 2a & b) suggest that the Altafjorden faults 1 & 2 contributed to the initial stages of formation of the NW Baltoscandian basins (Siedlecka et al., 2004; Nystuen et al., 2008) during the rifting of the Asgard Sea (Cawood et al., 2010; Cawood & Pisarevsky, 2017). Possible driving mechanisms for the formation of these basins and faults are a far-field influence of the coeval, basin-oblique/orthogonal, Sveconorwegian contraction, i.e. a formation as impactogenic rift-basins (Barberi et al., 1982), and/or a possible influence of late/post-orogenic collapse of the Sveconorwegian Orogeny (Bingen et al., 2008; Viola et al., 2013). The latest Mesoproterozoic-early Neoproterozoic ages (ca. 1050-945 Ma) obtained on illite in coarsest and intermediate fractions of brittle fault-rocks (Table 2, Figure 4 & Figure 5) suggest that basement rocks of the Alta-Kvænangen tectonic window were already exhumed above the brittle-ductile transition at that time, and may provide a maximum estimate for the age of quartz- and calcite-rich cataclasites formed at depth of 5-10 km along these faults (Figure 3b & c).

The finest fractions of both samples and intermediate fraction of sample 3 of non-cohesive fault-rocks in basement rocks yielded mid-Neoproterozoic ages (ca. 825-810 Ma; Table 2, Figure 4 & Figure 5). Combining these ages with normal shear-sense indicators observed in the field (Figure 2a & b), we propose that they represent the onset of rifting of the Iapetus Ocean-Ægir Sea during the breakup of Rodinia between 825 and 740 Ma (Torsvik & Rehnström, 2001; Hartz & Torsvik, 2002; Li et al., 2008). Similar Neoproterozoic K/Ar ages of ca. 790-780 Ma and 740-735 Ma are reported from dating of authigenic illite/muscovite along the Kvenklubben and Porsavannet faults in the adjacent Repparfjord-Komagfjord tectonic window in NW Finnmark (Torgersen et al., 2014; Figure).

The Altafjorden faults 1 & 2, although located close and oriented sub-parallel to Caledonian thrust faults (e.g. the Talvik fault; Figure 2e) and major, post-Caledonian normal faults (e.g. the LVF; Figure), were most likely not reactivated after ca. 810 Ma (mid-Neoproterozoic; Table 2, Figure 4 & Figure 5), as subsequent faulting would have triggered younger mineral assemblages and ages. Possible explanations for the non-reactivation of these faults include a north/westwards (basinwards?) migration of rifting to areas adjacent to the LVF, e.g. the Kvenklubben and Porsavannet faults dated at ca. 790-735 Ma (Torgersen et al., 2014), and to faults in Troms) and northern Finnmark, where Ediacaran metadolerite dykes intruded basement rocks during the breakup of the Iapetus Ocean-Ægir Sea (Zwaan

& van Roermund, 1980; Siedlecka et al., 2004; Nasuti et al., 2015). The lack of reactivation of Altafjorden faults 1 & 2, predominance of authigenic smectite clay mineral in non-cohesive fault-rock (samples 3 & 4 in Table 1 & Appendix 1) and the irreversibility of smectite-illite transformation (Eberl et al., 1993) suggest that Precambrian rocks of the Alta-Kvænangen tectonic window were exhumed and have remained at shallow depth < 3.5 km since the mid-Neoproterozoic (ca. 825 Ma; Table 2, Figure 4 & Figure 5). This conclusion is supported by predominance and preservation of authigenic smectite in similar non-cohesive fault-rocks in the Repparfjord-Komagfjord tectonic window (Torgersen et al., 2014).

Exhumation rates during latest Mesoproterozoic-early Neoproterozoic normal faulting are unknown. However, exhumation rate from the early (ca. 945 Ma and 5-10 km depth) to mid-Neoproterozoic (ca. 825 Ma and 1-3.5 km depth) were probably in the range of ca. 10-75 m per Ma, i.e. comparable to what is expected from average continental erosion rates (10-100 m per Ma; Schaller et al., 2002; Eppes & Keanini, 2017 – their figure 5). This therefore suggests a period of tectonic quiescence between opening of the Asgard Sea (first two, quartz/calcite-rich faulting events) and the onset of Iapetus rifting (final, smectite-rich faulting event).

5.2. Phanerozoic faulting and exhumation history

5.2.1.Evolution of temperature conditions in Caledonian rocks

We described five types of cohesive cataclastic fault-rocks in NW Finnmark based on mineralogical and textural descriptions. First, epidote- and chlorite-rich, stilpnomelane-bearing cataclasite (Figure 3e & h-j) formed by faulting of Caledonian mafic schists and gneisses (amphibolites; Figure 3d & e; Ramsay et al., 1979; 1985; Gayer et al., 1985)) and is consistently truncated by and incorporated into the other four types of cataclasites (Figure 3e & h-j), suggesting that epidote/chlorite-rich cataclasites correspond to the earliest stage of brittle faulting recorded by Caledonian rocks. The epidote + chlorite + stilpnomelane ± biotite mineral assemblages present both in the epidote/chlorite-rich cataclasites and adjacent host rocks, where biotite is almost completely recrystallized into chlorite (Figure 3d), indicate lower greenschist facies conditions during this faulting event, which constrain the minimum temperature during faulting to ca. 300°C (i.e. 10 km depth). Further, rounded clasts of stilpnomelane in epidote-rich cataclastic veins onshore Magerøya (Figure 3h & k) suggest faulting temperatures at prehnite-pumpellyite to lower greenschist facies conditions comprised between 300°C and 470°C (Miyano & Klein, 1989), i.e. a depth range of 10-16 km.

The second type of cataclasite corresponds to very fine-grained, quartz-rich cataclasite and veins of recrystallized quartz that often truncate and incorporate clasts of (type 1) epidote- and chlorite-rich cataclastic veins (Figure 3e & h). Since quartz dissolution only occurs at temperatures > 90°C (Worley & Tester, 1995) and deforms plastically at temperature > 300°C (Scholz 1988; Hirth & Tullis, 1989),

we argue that the quartz-rich cataclasite and associated quartz veins were formed during a discrete, second faulting event at depth comprised between 3 and 10 km. The transition from early, deep (10-16 km), epidote/chlorite-rich faulting to subsequent, shallower (3-10 km) quartz-rich cataclasis indicates that Caledonian rocks were partly exhumed between the two faulting events.

The third type of cataclasite is made up of widespread calcite both as clasts, cement and precipitations (Figure 3e & i). This type of cataclasite crosscuts epidote/chlorite- (type 1) and quartz-rich cataclasites (type 2), hence suggesting calcite-rich cataclasite (type 3) formed during a younger (reactivation) faulting event (Figure 3e & i). Since calcite crystals of the cataclasite display characteristic twinning type I and II (Figure 3i), we inferred a temperature range of 150-200°C (Lerman, 1999) and a depth of 5-7 km during this tentative, third faulting event.

A fourth type of cataclasite is present along fault segments of the LVF and TKFZ, showing pervasive laumontite clasts and precipitations (Figure 3m), and consistently truncates greenschist facies cataclasites (types 1, 2 & 3). Laumontite crystals are commonly undeformed and often appear as elongated crystals with their long axis perpendicular to fracture boundaries (Figure 3m). These observations suggest that laumontite formed as late growth along opening extensional cracks or in tension veins, most likely at a later stage of faulting than minerals in the greenschist facies cataclasites. Laumontite crystals themselves often appear mildly cataclased (Figure 3e, l & m), thus indicating that faulting persisted after the growth of laumontite. The temperature stability range of laumontite is 50-230°C (Jové & Hacker, 1997), which suggests that syn/post-laumontite faulting occurred at a depth range of ca. 2-8 km, i.e. probably shallower than faulting event associated with epidote/chlorite- (type 1), quartz- (type 2) and calcite-rich (type 3) cataclasites.

The fifth type of cataclasite is composed of iron oxide and clay minerals that crosscut all other cataclasite types and vein minerals (Figure 3h, l & n). XRF analyses of related non-cohesive fault-rock show a consistent dominance of authigenic smectite with subsidiary mixed-layer chlorite-smectite and minor illite (Table 1 & Appendix 1), suggesting the dominant clay mineral observed in the fifth type of cohesive cataclastic fault-rocks is smectite. Based on the preservation of abundant authigenic smectite (cf. Table 1 & Appendix 1) and on the irreversibility of the smectite-illite diagenetic transformation (Eberl et al., 1993), we propose that the ultimate (fifth) faulting event(s) in Caledonian rocks in NW Finnmark occurred at temperatures < 105°C (Morley et al., 2018), i.e. depth < 3.5 km, and that Caledonian rocks have remained at such shallow depth through Mesozoic-Cenozoic times.

Locally, XRF analysis of cohesive fault-rocks along WNW-ESE trending fault segments of the TKFZ in western Magerøya (sample 10; Figure) show almost pure authigenic smectite (Table 1 & Appendix 1). This constrains temperature during faulting to a minimum of 35-65°C (ca. 1-2 km depth) at which small amounts of illite may form (Eberl et al., 1993; Huang et al. 1993; Morley et al., 2018). Shallow faulting is further supported by the presence of mixed-layer chlorite-smectite clays (in samples 1, 2, 6 & 8; Table 1 & Appendix 1), which suggests that smectite (and mixed-layer chlorite-smectite) authigenic clays formed by retrograde diagenesis (i.e. exhumation) of crushed chlorite during faulting

(Warr & Cox, 2001; Nieto et al., 2005; Haines & van der Pluijm, 2012). Thus, we argue that Caledonian rocks along the LVF and TKFZ experienced another (late-stage) phase of uplift/faulting and exhumation from zeolite facies conditions (2-8 km) to diagenetic conditions (1-3.5 km). Alternatively, chlorite-smectite in non-cohesive fault-rocks along fault-segments of the LVF (e.g. samples 1 & 2; Figure , Table 1 & Appendix 1) formed during the shallowest phase of smectite-illite clay mineral reaction, while interlayered illite-smectite (cf. sample 8; Table 1 & Appendix 1) formed during deeper phases of this reaction due to higher, normal faulting-related burial in the hanging-wall of the LVF (Whitney & Northrop, 1988). However, more samples are needed in the hanging-wall of the LVF to verify this hypothesis (only sample 8; Figure).

5.2.2.Timing of Phanerozoic faulting and exhumation of Caledonian rocks

Late Paleozoic inversion of brittle-ductile Caledonian thrusts

The coarse fraction of the Talvik fault (sample 5; Figure), a south-verging Caledonian thrust in rocks of the Kalak Nappe Complex in Altafjorden, yielded a mid/late Silurian age (427.3 ± 8.4 Ma) suggesting that brittle faulting along this fault initiated during the latest stages of the Caledonian Orogeny (Table 2, Figure 4 & Figure 6). Movement along the Talvik fault started with top-to-the-south, ductile Caledonian thrusting as shown by quartz sigma-clasts and shear bands in mylonitic foliation, likely at a depth > 10 km (Scholz, 1988; Hirth & Tullis, 1989), and continued with down-to-the-north, brittle, normal dip-slip faulting truncating ductile fabrics (Figure 2e). The earliest evidence of late/post-Caledonian, normal faulting in northern Norway are Early Devonian ages obtained for inverted shear zones in Vesterålen (Steltenpohl et al., 2011). This suggests that the mid/late Silurian faulting age/event recorded along the Talvik fault (coarse fraction) might represent a phase of top-to-the-south, brittle (-ductile?), Caledonian thrusting, rather than late/post-Caledonian normal faulting (Figure 2e). Exhumation of the Talvik fault to brittle depth < 10 km in the mid/late Silurian was most likely due to combined thrusting and erosion. Alternatively, this Silurian age reflects input from inherited illite/muscovite component as shown by a small illite peak with epizonal KI (< 0.25) in the coarse fraction of this sample (Appendix 1), suggesting a faulting event younger than the Silurian.

Top-to-the-south, Silurian, brittle thrusting along the Talvik fault was followed by successive early Carboniferous (Tournaisian), 353.7 ± 4.1 Ma and early Permian, 282.1 ± 6.3 Ma faulting events obtained from the intermediate and finest gouge fractions respectively (Table 2, Figure 4 & Figure 6). These events likely reflect post-Caledonian, down-to-the-N reactivation as a normal fault during the collapse of the Caledonides. Extensional reactivation is supported by normal dip-slip slickensides along the Talvik fault truncating the initial ductile fabrics (Figure 2e). Further support appears from the early Permian inversion of an analog Caledonian thrust in the Repparfjord-Komagfjord tectonic window, the Kvenklubben fault (Torgersen et al., 2014), and from offshore seismic studies on the Finnmark Platform,

where a major Caledonian thrust, the Sørøya-Ingøya shear zone, was inverted in the Mid/Late Devonian-early Carboniferous (Figure ; Koehl et al., 2018).

Late Paleozoic normal faulting

Our dating efforts of brittle segments of the LVF and TKFZ outlined above revealed numerous and consistent, late Paleozoic ages (Table 2, Figure 4 & Figure 6). Obtained K-Ar ages cover a time span from early Carboniferous (Tournaisian; one age) for the Talvik fault, late Carboniferous (three ages) for brittle faults on the Porsanger Peninsula and Magerøya (samples 8, 9 & 10; Figure 4 & Figure 6), to early-mid Permian (eight ages for samples 5, 6, 8, 9 & 10; Figure 4 & Figure 6). By comparison, early (four ages) to late (one age) Carboniferous K-Ar ages were reported for the Markopp fault, and (two) early Permian ages for the Kvenklubben fault in nearby rocks of the Repparfjord-Komagfjord tectonic window (Torgersen et al., 2014). In addition, the Laksvatn fault in Western Troms (Figure) yielded two Late Devonian ages (Davids et al. 2013). This down-to-the-NW normal fault is interpreted as a major, inverted Caledonian thrust possibly merging with the southwestern continuation of the LVF (Koehl et al., submitted), thus suggesting that post-Caledonian, normal brittle faulting along the LVF initiated in the Late Devonian. Further support of Devonian faulting is found offshore, where potential Mid/Late Devonian sedimentary rocks were deposited along inverted Caledonian thrusts on the Finnmark Platform west, and where the offshore segments of the LVF on the Finnmark Platform east (Koehl et al., 2018) bound a major (half-) graben filled with Carboniferous (Bugge et al., 1995) and, conceivably, latest Devonian clastic sedimentary deposits (Roberts et al., 2011).

The dated faults in the Porsanger Peninsula (sample 8; Figure 2h), Talvik (sample 5; Figure 2e) and Storekorsnes (sample 6; Figure 2f) show down-to-the-north, normal dip-slip to oblique-slip movements, suggesting that they are all related to late Paleozoic, post-Caledonian extension. The long time-spread of the obtained late Paleozoic, post-Caledonian K/Ar ages (Table 2, Figure 4 & Figure 6) suggests either a long-term progressive, or two discrete faulting periods. From our results, we favor two discrete periods, one in the Late Devonian-early Carboniferous at ca. 375-325 Ma (based on one age in this study, four from Torgersen et al., 2014 and two from Davids et al., 2013) and one in the late Carboniferous-mid Permian at ca. 315-265 Ma (eleven ages from the present study and two from Torgersen et al., 2014).

The obtained earliest Permian (Asselian) ages for three different fractions of the same cataclasite in the fault in the hanging-wall of the LVF on the Porsanger Peninsula (sample 8, Figure , Table 2, Figure 4 & Figure 6), verified within two-sigma error range, may reflect a single faulting event. The short time span suggests that the fault was not reactivated later, since further faulting would have been recorded in the finest grainsize fraction. This conclusion is supported by offshore seismic data on the Finnmark Platform, showing that the thickness of Permian sedimentary rocks is constant across brittle normal faults, such as the LVF and Måsøy Fault Complex (Figure), and that most brittle faults die out within the Carboniferous and lower part of the Permian sedimentary successions (Koehl et al., 2018).

However, offshore seismic data on the Finnmark Platform suggest that early-mid Permian, K/Ar ages (Table 2, Figure 4 & Figure 6 and Torgersen et al., 2014) obtained onshore NW Finnmark may represent only minor tectonic adjustments rather than major faulting events (Koehl et al., 2018). Thus, an alternative interpretation for the dominance of Permian ages is due to partial overprinting/resetting of authigenic illite from the main early (-late?) Carboniferous faulting period.

Of the five dated faults that yielded late Paleozoic, post-Caledonian ages (samples 5, 6, 8, 9 & 10; Table 2 & Figure 4), only two of them included cohesive fault-rock (samples 5 & 6; Figure). For those that only comprised non-cohesive gouge (samples 8, 9 & 10) with predominance of authigenic smectite clay mineral and subsidiary authigenic illite (Table 1 & Appendix 1), it seems reasonable to conclude that faulting occurred at shallow depth between 1-3.5 km (Eberl et al., 1993; Morley et al., 2018) in the late Carboniferous-mid Permian (Figure 4 & Figure 6). The other two faults that yielded late Paleozoic ages (samples 5 & 6; Figure) and comprise both cohesive and non-cohesive fault-rocks (Figure 2e & f), likely formed at deeper crustal levels and higher p/T conditions. Non-cohesive fault-rocks along the Talvik fault (sample 5), consisting of authigenic smectite with minor illite, yielded early Carboniferous (intermediate fraction) and early Permian (finest fraction) ages (Table 2), while cohesive fault-rocks along this fault are characterized by both quartz- and calcite-rich cataclasites (types 2 & 3). These data, backed by crosscutting relationships between quartz-, calcite- and clay-rich cohesive fault-rocks (types 2, 3 & 5; Figure 3e), suggest that quartz- and calcite-rich cataclasites (types 2 & 3) along the Talvik fault formed in the Late Devonian (?) - early Carboniferous at a depth range of ca. 3-10 km (Scholz, 1988; Hirth & Tullis, 1989; Worley & Tester, 1995; Lerman, 1999). Later on, these cataclasites were overprinted by non-cohesive, smectite-rich, cohesive (type 5) and non-cohesive fault-rocks generated at depth of 1-3.5 km in the early Permian (Figure 6; Eberl et al., 1993; Morley et al., 2018). These data are consistent with a partial exhumation of the Talvik fault and nearby Caledonian host rocks from the early Carboniferous to early Permian, with average exhumation rate along this fault varying from < 185 (Silurian-early Carboniferous) to < 125 m per Ma (early Carboniferous-early Permian).

Similarly, for the fault in Storekorsnes, the intermediate and finest fractions of smectite-dominated, fault-gouge sample 6 (Figure , Table 1 & Appendix 1) yielded latest Carboniferous-early Permian ages (Table 2 & Figure 4), and the fault comprises epidote- (type 1), quartz- (type 2), zeolite- (type 4) and smectite/chlorite-smectite rich (type 5) cohesive fault-rocks (Figure 3e). The obtained K/Ar ages, kinematic, down-to-the-NW, normal dip-slip character (Figure 2f) and stability field of smectite suggest that smectite- and chlorite/smectite-rich cohesive and non-cohesive fault-rocks found along this fault formed during normal faulting in the latest Carboniferous-early Permian at depth of 1-3.5 km (Eberl et al., 1993; Morley et al., 2018). Epidote-rich and stilpnomelane-bearing (type 1), and quartz- (type 2) and zeolite-rich (type 4) cataclasites are all crosscut by smectite-rich (cohesive and non-cohesive) fault-rocks (Figure 3e) and reflect deeper faulting depths (ca. 2-10 km; Scholz, 1988; Hirth & Tullis, 1989; Miyano & Klein, 1989; Worley & Tester, 1995; Jové & Hacker, 1997; Lerman, 1999). Thus, we propose that cataclasites type 1, 2 and 4 formed much earlier, possibly in the Late Devonian-

early Carboniferous as suggested by K/Ar dating along the Laksvatn (Davids et al., 2013) and Talvik fault (Table 2 & Figure 4), and were later exhumed and overprinted by late Carboniferous-early Permian, smectite-rich faulting. Tentative driving mechanisms for exhumation may have been an interplay between normal faulting, footwall uplift and continental erosion. This is supported by extensive normal faulting offshore, in (Late Devonian?) Carboniferous rocks, and by the presence of a major, mid-Carboniferous erosional unconformity of pre-Pennsylvanian rocks on the Finnmark Platform (Larssen et al., 2002; Koehl et al., 2018).

Of importance in restoring the exhumation history of NW Finnmark is that authigenic smectite is particularly dominant in non-cohesive fault-rocks in the footwall and along fault segments of the LVF, although often associated to high amounts of chlorite along fault segments of the LVF (e.g. Talvik fault and Sørkjosen faults; see samples 1, 2 & 5 in Table 1 & Appendix 1), whereas interlayered illite-smectite dominates in non-cohesive fault-rocks in the hanging-wall of the LVF, e.g. sample 8 (cf. Figure , Table 1 & Appendix 1). A plausible interpretation is that km-scale, post-Caledonian downthrow to the northwest along the LVF (partly) enhanced the exhumation of brittle faults and Caledonian rocks in the footwall, while hanging-wall segments of the LVF remained at deeper levels, producing interlayered illite-smectite (cf. sample 8; Table 1 & Appendix 1), a deeper end-member product of the smectite-illite reaction (Whitney & Northrop, 1988). This conclusion may be partly falsified by the illite-smectite rich composition of fault-gouges along the Porsavannet and Markopp faults in the footwall of the LVF (Torgersen et al., 2014). However, these faults yielded significantly older ages (respectively mid Neoproterozoic-mid Paleozoic and early Carboniferous) than the late Carboniferous-early/mid Permian ages of smectite/chlorite-smectite rich fault-rocks from our study (Table 2). It is therefore possible that the authigenic, interlayered illite-smectite in fault-rocks along the Porsavannet and Markopp faults reflect earlier, deeper faulting periods.

Furthermore, XRF analyses of fault gouge from a segment of the TKFZ in western Magerøya (sample 10; Figure & Figure 2j), yielding late Carboniferous to mid-Permian K-Ar ages (cf. Table 2, Figure 4 & Figure 6), show almost pure authigenic smectite (cf. Table 1 & Appendix 1). This suggests that Permian faulting occurred at very low temperature of 35-65°C (Eberl et a., 1993; Huang et al., 1993; Morley et al. 2018), i.e. depth of ca. 1-2 km, and remained at shallow crustal levels until present, thus preventing transformation of smectite to illite through diagenesis. Late Paleozoic exhumation and shallow faulting in NW Finnmark and along other portions of the Barents Sea margin, e.g. Lofoten-Vesterålen, are supported by Apatite Fission Track data, indicating that outcropping rocks northern Norway have remained at relatively low temperature < 120°C, i.e. depth < 4 km, since mid-Permian times (Hendriks et al., 2007).

Considering K/Ar ages obtained on non-cohesive fault-rocks, and mineral assemblages and crosscutting relationships of the five types of cohesive fault-rocks, we estimate exhumation rates from the Silurian (ca. 425 Ma and 10-16 km depth) to Late Devonian (ca. 375 Ma and minimum 5-10 km depth) to be < 220 m per Ma, i.e. analogous to estimate along the Talvik fault (< 185 m per Ma).

Similarly, exhumation rates through the Late Devonian (ca. 375 Ma and minimum 5-10 km depth) - early Carboniferous (ca. 325 Ma and 2-8 km depth) faulting period were < 160 m, and < 115 m per Ma through the ultimate faulting period from the end of the early Carboniferous (ca. 325 Ma and maximum 2-8 km depth) to the mid-Permian (ca. 265 Ma and 1-3.5 km depth), i.e. similar to exhumation rates obtained along the Talvik fault (< 125 m per Ma). Decreasing exhumation rate from Silurian to mid-Permian times might indicate progressively milder faulting activity along the margin, with exhumation rates in the late Carboniferous-mid Permian being comparable/slightly higher than average continental erosion rates thought to be in the order of 10-100 m per Ma (Schaller et al., 2002; Eppes & Keanini, 2017 – their figure 5). Thus, we propose that exhumation in the Silurian-early Carboniferous was driven by a combination of continental erosion, thrusting and, later on, normal faulting, while exhumation in the late Carboniferous-mid Permian was mostly due to continental erosion with limited contribution of normal faulting.

Alternatively, the predominance of Permian faulting ages obtained onshore NW Finnmark may be attributed to a period of extensive weathering in the (late Carboniferous- ?) early-mid Permian (cf. Table 2, Figure 4 & Figure 6), possibly reflected by highly weathered host rocks and brittle fault surfaces showing no kinematic indicators onshore Magerøya (sample 9 & 10; Figure and Figure 2i & j). Although this weathering may be related to much younger processes (Olesen et al., 2012; 2013), Carboniferous-Permian, (sub-) tropical climate conditions prevailed in Baltica (Stemmerik, 2000; Larssen et al., 2002; Samuelsberg et al., 2003) and, hence, may have initiated weathering of exposed, uplifted footwall blocks along major faults like the LVF and Måsøy and Troms-Finnmark fault complexes offshore (Figure). This is supported by widespread exhumation and erosional truncation of pre-Pennsylvanian rocks in the footwall of the Troms-Finnmark Fault Complex, on the Finnmark Platform (Koehl et al., 2018), linked to a mid-Carboniferous phase of eustatic sea-level fall (Saunders & Ramsbottom, 1986). This exhumation/weathering event is also consistent with the Early Mesozoic, minimum age estimate of weathering of basement rocks along the Norwegian continental shelf (Olesen et al., 2012; 2013). Although the dated faults were still buried to depth > 1 km in the mid-Permian, as shown by the presence of (minor) authigenic illite (Eberl et al., 1993) used for K/Ar age dating of the faults, field studies in onshore tunnels in Norway show that weathering processes related to percolation of acidic water may penetrate the bedrock > 200 m along fault surfaces (Olesen et al., 2012; 2013), thus making this alternative explanation possible, though unlikely. Another obstacle to this interpretation is the lack of a major erosional unconformity/truncation in upper Carboniferous-lower/mid Permian sedimentary rocks on the Finnmark Platform offshore (Larssen et al., 2002; Samuelsberg et al., 2003; Koehl et al., 2018).

Mesozoic faulting

Reliable Mesozoic K/Ar age was only obtained for the finest fraction of the Snøfjorden-Slatten fault (sample 7; Figure & Table 2), yielding a Hettangian age. All the other faults yielding Mesozoic

ages (all three fractions in samples 1 & 2, coarse fraction of sample 6, coarse and intermediate fractions of sample 7 and intermediate fraction of sample 9) comprise subsidiary K-feldspar (Table 1 & Appendix 1), which provided additional potassium and, thus, yielded younger ages than the actual age of faulting (Table 2; cf. red ages in Figure 4). Thus, we disregard these ages because of their high uncertainty. Considering the scarsity of Mesozoic-Cenozoic ages, we argue that NW Finnmark, as well as adjacent offshore areas of the Finnmark Platform (Koehl et al., 2018) were tectonically quiet after late Paleozoic (Devonian-mid Permian) extension and were only subjected to minor, local extensional faulting events, e.g. in the earliest Jurassic (Hettangian) for the Snøfjorden-Slatten fault (cf. Figure , Table 2, Figure 4 & Figure 6) and Early Cretaceous for the Kvenklubben fault (Torgersen et al., 2014).

5.3. Regional implications

An implication of the latest Mesoproterozoic-Neoproterozoic K/Ar ages obtained for the ENE-WSW trending Altafjorden faults 1 & 2 in the Alta-Kvænangen tectonic window is that they partly support the interpretation of Koehl et al. (submitted), suggesting that ENE-WSW trending faults represent inherited Precambrian fault fabrics. However, the inferred normal sense of shear and latest Mesoproterozoic-mid Neoproterozoic K/Ar faulting ages obtained for the Altafjorden faults 1 & 2 (Figure 2a & b) suggest that these faults formed as extensional normal faults rather than conjugate strike-slip faults to WNW-ESE trending faults like the TKFZ as suggested by Koehl et al. (submitted). Instead, latest Mesoproterozoic-mid Neoproterozoic brittle faults might have provided preferentially oriented weakness zones for the formation of subparallel, subsequent and adjacent Caledonian thrusts (e.g. Talvik fault) and post-Caledonian normal faults (e.g. LVF; Figure). Nevertheless, conjugate strike-slip faults may exist in NW Finnmark (Roberts, 1971; Worthing, 1984), but these display subvertical geometries and significant lateral displacement, and may have formed during E-W/ENE-WSW directed, Timanian contraction in the late Neoproterozoic, e.g. TKFZ (Siedlecka et al., 2004; Herrevold et al., 2009) and Akkarfjord fault (Roberts, 1971; Koehl et al., submitted).

Analogous studies of post-Caledonian brittle faults in Western Troms show that post-Caledonian extensional faulting initiated at depth > 10 km at greenschist facies conditions and continued under pumpellyite-prehnite facies conditions at depth < 8.5 km, thus supporting a gradual exhumation of the margin (Indrevær et al., 2013, 2014). More detailed mineralogic-textural analysis of clay-rich non-cohesive fault-rocks of the Vannareid-Burøysund, Sifjord and Laksvatn faults revealed dominance of smectite and chlorite clay minerals (Davids et al. 2013), suggesting that brittle faults in Western Troms were exhumed to low temperature conditions (35-105°C; Eberl et al., 1993; Morley et al., 2018) and shallow depths (1-3.5 km) comparable the LVF and TKFZ in NW Finnmark. Furthermore, fault-gouge along the SSE-dipping Vannareid-Burøysund and Sifjord faults yielded similar early Carboniferous (intermediate fractions) and early Permian K/Ar ages (finest fractions; Davids et al.,

2013) compatible with the proposed Late Devonian-early Carboniferous and late Carboniferous-mid Permian stages of post-Caledonian brittle faulting in NW Finnmark (Table 2, Figure 4, Figure 6 and Torgersen et al., 2014).

A major contrast in K/Ar ages in Western Troms and NW Finnmark is occurrence of latest Mesoproterozoic-mid Neoproterozoic ages for gouges of the southeasternmost normal faults within basement rocks of the Alta-Kvænangen tectonic window in NW Finnmark (Figure 4 & Figure 5), while analogous faults in Archean-Paleoproterozoic rocks of the West Troms Basement Complex (Zwaan, 1995; Bergh et al., 2010) yielded Carboniferous-Permian ages (Davids et al., 2013). Another mild contrast is the occurrence of slightly younger, late Permian-Early Triassic, K/Ar faulting ages for brittle faults in Western Troms (Davids et al., submitted), suggesting that extension migrated westwards after the late Carboniferous-mid Permian and persisted until the Early Triassic in coastal areas of Western Troms. Westwards younging of K/Ar faulting ages is further supported by Mesozoic ages obtained for three faults in western Lofoten (Davids et al., 2013). Nonetheless, widespread Late Devonian-early Carboniferous and late Carboniferous-mid Permian ages in NW Finnmark, Western Troms and Lofoten-Vesterålen suggest that the main episode of extension and exhumation along the margin occurred in the late Paleozoic and was probably related to the collapse of the Caledonides (Davids et al., 2013, submitted; Torgersen et al., 2014; Koehl et al., 2018). Apatite Fission Track data in Western Troms and Lofoten-Vesterålen also indicate a period of rapid cooling (1-2°C/Ma) in the late Paleozoic, possibly due to combined extensive normal faulting and erosion, followed by a period of relatively slow cooling (< 0.2°C/Ma) in Mesozoic times, likely suggesting a tectonically quiet time period (Davids et al., 2013).

6. Conclusions

1) Three faulting events occurred in the latest Mesoproterozoic-mid Neoproterozoic (ca. 1050-810 Ma), including (i) latest Mesoproterozoic faulting (ca. 1050 Ma.) and (ii) an early Neoproterozoic faulting event (ca. 945 Ma) with quartz-rich and calcite-cemented cataclasites formed at depth of ca. 5-10 km, possibly reflecting the formation of the NW Baltoscandian basins during the opening of the Asgard Sea, and (iii) a shallow (depth 1-3.5 km), mid-Neoproterozoic faulting episode (ca. 825-810 Ma) with abundant authigenic smectite, related to the opening of the Iapetus Ocean-Ægir Sea and breakup of Rodinia between 825-740 Ma.

2) Exhumation rates estimates from 945 to 825 Ma were in the order of 10-75 m per Ma, thus indicating that continental erosion alone may account for early-mid Neoproterozoic exhumation and that tectonic quiescence prevailed between the opening of the Asgard Sea and the opening of the Iapetus Ocean-Ægir Sea.

3) The preservation of abundant authigenic smectite in cohesive and non-cohesive fault-rocks suggests that Paleoproterozoic basement rocks were exhumed to and remained at shallow crustal levels (< 3.5

km depth) since the mid-Neoproterozoic (ca. 825 Ma), and were not reactivated after mid-Neoproterozoic times despite being oriented parallel to major Caledonian thrusts and post-Caledonian normal faults.

4) Five faulting events occurred in Caledonian rocks, defining three faulting periods: (i) potential Silurian, top-to-the-south thrusting along Caledonian thrusts (e.g. Talvik fault) initiated at a depth of 10-16 km, and was possibly associated with epidote/chlorite-rich, stilpnomelane-bearing cataclasis (type 1), (ii) widespread, Late Devonian-early Carboniferous (ca. 375-325 Ma) extensional faulting, occurred at decreasing depth and was accompanied by quartz-rich (type 2; 3-10 km depth), calcite-cemented (type 3; 5-7 km depth) and laumontite-rich cataclasites (type 4; 2-8 km depth) formed during three discrete faulting events possibly related to the collapse of the Caledonides, (iii) an ultimate, minor stage of shallow faulting in the late Carboniferous-mid Permian (ca. 315-265 Ma) dominated by iron/smectite/chlorite-smectite rich, illite-bearing (type 5) fault-rocks formed at depth of 1-3.5 km, thus suggesting Caledonian rocks were progressively exhumed to near-surface depth in late Paleozoic times.

5) Km-scale, down-to-the-NW normal faulting and footwall uplift along the Langfjord-Vargsund fault may be responsible for local variation of dominant, authigenic clay minerals in type 5 fault-rocks (1-3.5 km depth), producing deeper, interlayered illite-smectite in the hanging-wall and shallower, smectite and mixed-layer chlorite-smectite in the footwall.

6) Decreasing exhumation rates, < 220 m per Ma in Silurian-Late Devonian (425-375 Ma), < 160 m per Ma in Late Devonian-early Carboniferous (375-325 Ma) and < 115 m per Ma from mid-Carboniferous to mid-Permian times (325-265 Ma), suggest a transition from extensive, widespread Caledonian thrusting and collapse-related normal faulting to milder normal faulting in the late Carboniferous-mid Permian. The high number of early-mid Permian, K/Ar ages may, alternatively, reflect an episode of (near-) surface weathering in NW Finnmark. Subsequent Mesozoic-Cenozoic extension migrated westwards and NW Finnmark remained tectonically quiet from the mid-Permian.

Acknowledgements

The present study is part of the ARCEx project (Research Centre for Arctic Petroleum Exploration), which is funded by the Research Council of Norway (grant number 228107) together with ten academic and eight industry partners. We would like to thank all the persons from these institutions that are involved in this project. We acknowledge the contribution of student research assistants from the K/Ar laboratory at the University of Göttingen for their work preparing and analyzing the samples of non-cohesive fault-rock presented in this study. Finally, the authors would like to thank Anna Ksienzyk from the University of Bergen for fruitful discussions.

References

Andersen, T. B.: The structure of the Magerøy Nappe, Finnmark, North Norway, Nor. geol. unders., 363, 1-23, 1981.

Andersen, T. B.: The stratigraphy of the Magerøy Supergroup, Finnmark, north Norway, Nor. geol. unders., 395, 25-37, 1984.

Bergh, S. G. and Torske, T.: The Proterozoic Skoadduvarri Sandstone Formation, Alta, Northern Norway: A tectonic fan-delta complex, Sedimentary Geology, 47, 1-25, 1986.

Bergh, S. G. and Torske, T.: Palaeovolcanology and tectonic setting of a Proterozoic metatholeiitic sequence near the Baltic Shield Margin, northern Norway, Precambrian Research, 39, 227-246, 1988.

Bergh, S. G., Eig, K., Kløvjan, O. S., Henningsen, T., Olesen, O. and Hansen, J-A.: The Lofoten-Vesterålen continental margin: a multiphase Mesozoic-Palaeogene rifted shelf as shown by offshore-onshore brittle fault-fracture analysis, Norwegian Journal of Geology, 87, 29-58, 2007.

Bergh, S. G., Kullerud, K., Armitage, P. E. B., Zwaan, K. B., Corfu, F., Ravna, E. J. K. and Myhre, P. I.: Neoarchean to Svecofennian tectono-magmatic evolution of the West Troms Basement Complex, North Norway, Norwegian Journal of Geology, 90, 21-48, 2010.

Bergø, E.: Analyses of Paleozoic and Mesozoic brittle fractures in West-Finnmark, Unpublished Master's Thesis, University of Tromsø, 128 pp., 2016.

Bingen, B., Nordgulen, Ø. And Viola, G.: A four-phase model for the Sveconorwegian orogeny, SW Scandinavia, Norwegian Journal of Geology, 88, 43-72, 2008.

Bugge, T., Mangerud, G., Elvebakk, G., Mørk, A., Nilsson, I., Fanavoll, S. and Vigran, J. O.: The Upper Palaeozoic succession on the Finnmark Platform, Barents Sea, Norsk Geologisk Tidsskrift, 75, 3-30, 1995.

Breivik, A. J., Gudlaugsson, S. T. and Faleide, J. I.: Ottar Basin, SW Barents Sea: a major Upper Palaeozoic rift basin containing large volumes of deeply buried salt, Basin Research, 7, 299-312, 1995.

Bøe, P. and Gautier, A. M.: Precambrian primary volcanic structures in the Alta-Kvænangen tectonic window, northern Norway, Norsk Geologisk Tidsskrift, 58, 113-119, 1978.

Cawood, P. A. and Pisarevsky, S. A.: Laurentia-Baltica-Amazonia relations during Rodinia assembly, Precambrian Research, 292, 386-397, 2017.

Cawood, P. A., Strachan, P., Cutts, K., Kinny, P. D., Hand, M. and Pisarevsky, S.: Neoproterozoic orogeny along the margin of Rodinia: Valhalla orogeny, North Atlantic, Geology, 38, 99-102, 2010.

Corfu, F., Torsvik, T. H., Andersen, T. B., Ashwal, L. D., Ramsay, D. M. and Roberts, R. J.: Early Silurian mafic-ultramafic and granitic plutonism in contemporaneous flysch, Magerøy, northern

Norway: U-Pb ages and regional significance, Journal of the Geological Society, London, 163, 291-301, 2006.

Corfu, F., Andersen, T. B. and Gasser, D.: The Scandinavian Caledonides: main features, conceptual advances and critical questions, in: New Perspectives on the Caledonides of Scandinavia and Related Areas, Corfu, F., Gasser, D. and Chew, D. M. (eds), Geological Society, London, Special Publications, 390, 9-43, 2014.

Davids, C., Wemmer, K., Zwingmann, H., Kohlmann, F., Jacobs, J. and Bergh, S. G.: K-Ar illite and apatite fission track constraints on brittle faulting and the evolution of the northern Norwegian passive margin, Tectonophysics, 608, 196-211, 2013.

Davids, C., Benowitz, J. E., Layer, P. W. and Bergh, S. G.: Direct $^{40}Ar/^{39}Ar$ feldspar dating of Late Permian – Early Triassic brittle faulting in northern Norway, Terra Nova, submitted.

Dill, H. G., Füßl, M. and Botz, R.: Mineralogy and (economic) geology of zeolite-carbonate mineralization in basic igneous rocks of the Troodos Complex, Cyprus, N. Jb. Miner. Abh., 183/3, 251-268, 2007.

Eberl, D. D., Velde, B. and McCormick, T.: Synthesis of illite-smectite from smectite at Earth surface temperatures and high pH, Clay Minerals, 28, 49-60, 1993.

Eggleton, R. A.: The crystal structure of stilpnomelane. Part II. The full cell, Mineralogical Magazine, 38, 693-711, 1972.

Eig, K. and Bergh, S. G.: Late Cretaceous-Cenozoic fracturing in Lofoten, North Norway: Tectonic significance, fracture mechanisms and controlling factors, Tectonophysics, 499, 190-215, 2011.

Elvevold, S., Reginiussen, H., Krogh, E. J. and Bjørklund, F.: Reworking of deep-seated gabbros and associated contact metamorphosed paragneisses in the south-eastern part of the Seiland Igneous Province, northern Norway, Journal of Metamorphic Geology, 12, 539-556, 1994.

Eppes, M-C. and Keanini, R.: Mechanical weathering and rock erosion by climate-dependent subcritical cracking, Rev. Geophys., 55, 470-508, 2017.

Faleide, J. I., Vågnes, E. and Gudlaugsson, S. T.: Late Mesozoic-Cenozoic evolution of the south-western Barents Sea in a regional rift-shear tectonic setting, Marine and Petroleum Geology, 10, 186-214, 1993.

Faleide, J. I., Tsikalas, F., Breivik, A. J., Mjelde, R., Ritzmann, O., Engen, Ø., Wilson, J. and Eldholm, O.: Structure and evolution of the continental margin off Norway and the Barents Sea, Episodes, 31, 82-91, 2008.

Fuhrmann, U., Lippolt, H. J. and Hess, J. C.: Examination of some proposed K-Ar standards: $^{40}Ar/^{39}Ar$ analyses and conventional K-Ar-Data, Chem. Geol. (Isot. Geosci. Sect.), 66, 41-51, 1987.

Gabrielsen R. H., Færseth, R. B., Jensen, L. N., Kalheim, J. E. and Riis, F.: Structural elements of the Norwegian continental shelf, Part I: The Barents Sea Region, Norwegian Petroleum Directorate Bulletin, 6, 33 pp., 1990.

Gautier, A. M., Zwaan, K. B., Bakke, I., Lindahl, I., Ryghaug, P. and Vik, E.: KVÆNANGEN berggrundskart 1734 1, 1:50 000, foreløpig utgave, Nor. geol. unders., 1987.

Gayer, R. A., Hayes, S. J. and Rice, A. H. N.: The structural development of the Kalak Nappe Complex of Eastern and Central Porsangerhalvøya, Finnmark, Norway, Nor. geol. unders. bull., 400, 67-87, 1985.

Gudlaugsson, S. T., Faleide, J. I., Johansen, S. E. and Breivik, A. J.: Late Palaeozoic structural development of the South-western Barents Sea, Marine and Petroleum Geology, 15, 73-102, 1998.

Haines, S. H. and van der Pluijm, B. A.: Patterns of mineral transformations in clay gouge, with examples from low-angle normal fault rocks in the western USA, Journal of Structural Geology, 43, 2-32, 2012.

Hamilton, P. J., Kelley, S. and Fallick, A. E.: K-Ar dating of illite in hydrocarbon reservoirs, Clay Minerals, 24, 215-231, 1989.

Hartz, E. H. and Torsvik, T. H.: Baltica upside down: A new plate tectonic model for Rodinia and the Iapetus Ocean, Geology, 30, 255-258, 2002.

Harvey C. and Browne, P.: Mixed-layer clays in geothermal systems and their effectiveness as mineral geothermometers, Proceedings Worls Geothermal Congress 2000, Kynshu – Tohoku, Japan, May 28 – June 10, 2000.

Heizler, M. T. and Harrison, T. M.: The heating duration and provenance age of rocks in the Salton Sea geothermal field, southern California, Journal of Volcanology and Geothermal Research, 46, 73-97, 1991.

Hendriks, B., Andriessen, P., Huigen, Y., Leighton, C., Redfield, T., Murrell, G., Gallagher, K. and Nielsen, S. B.: A fission track data compilation for Fennoscandia, Norwegian Journal of Geology, 87, 143-155, 2007.

Heinrichs, H. and Herrmann, A. G.: Praktikum der Analytischen Geochemie, Springer Verlag, 669 S., 1990.

Herrevold, T., Gabrielsen, R. H. and Roberts, D.: Structural geology of the southeastern part of the Trollfjorden-Komagelva Fault Zone, Varanger Peninsula, Finnmark, North Norway, Norwegian Journal of Geology, 89, 305-325, 2009.

Hirth, G. and Tullis, J.: The Effects of Pressure and Porosity on the Micromechanics of the Brittle-Ductile Transition in Quartzite, Journal of geophysical Research, 94, 17825-17838, 1989.

Huang, W-L., Longo, J. M. and Pevear, D. R.: An experimentally derived kinetic model for smectite-to-illite conversion and its use as a geothermometer, Clays and Clay Minerals, 41, 162-177, 1993.

Hunziker, J. C., Frey, M., Clauer, N., Dallmeyer, R. D., Friedrichsen, H., Flehmig, W., Hochstrasser, K., Roggwiler, P. and Schwander, H.: The evolution of illite to muscovite: mineralogical and

isotopic data from the Glarus Alps, Switzerland, Contributions to Mineralogy and Petrology, 92, 157-180,1986.

Indrevær, K., Bergh, S. G., Koehl, J-B., Hansen, J-A., Schermer, E. R. and Ingebrigtsen, A.: Post-Caledonian brittle fault zones on the hyperextended SW Barents Sea margin: New insights into onshore and offshore margin architecture, Norwegian Journal of Geology, 93, 167-188, 2013.

Indrevær, K., Stunitz, H. and Bergh, S. G.: On Palaeozoic-Mesozoic brittle normal faults along the SW Barents Sea margin: fault processes and implications for basement permeability and margin evolution, Journal of the Geological Society, London, 171, 831-846, 2014.

Jennings, S. and Thompson, G. R.: Diagenesis of Plio-Pleistocene sediments of the Colorado River Delta, southern California, Journal of Sedimentary Petrology, 56, 89-98, 1986.

Jensen, P. A.: The Altenes and Repparfjord tectonic windows, Finnmark, northern Norway: Remains of a Palaeopreterozoic Andean-type plate margin at the rim of the Baltic Shield, Unpublished Ph.D. Thesis, University of Tromsø, 1996.

Jové, C. and Hacker, B. R.: Experimental investigation of laumontite → waraikite + H_2O: A model diagenetic reaction, American Mineralogist, 82, 781-789, 1997.

Kirkland, C. L., Daly, J. S. and Whitehouse, M. J.: Early Silurian magmatism and the Scandian evolution of the Kalak Nappe Complex, Finnmark, Arctic Norway, Journal of the Geological Society, London, 162, 985-1003, 2005.

Kirkland, C. L., Daly, J. S. and Whitehouse, M. J.: Provenance and Terrane Evolution of the Kalak Nappe Complex, Norwegian Caledonides: Implications for Neoproterozoic Paleogeography and Tectonics, The Journal of Geology, 115, 21-41, 2007.

Kirkland, C. L., Daly, J. S. and Whitehouse, M. J.: Basement-cover relationships of the Kalak Nappe Complex, Arctic Norwegian Caledonides and constraints on Neoproterozoic terrane assembly in the North Atlantic region, Precambrian Research, 160, 245-276, 2008.

Kisch, H. J.: Illite „crystallinity“: recommendations on sample preparation, X-ray diffraction settings and inter-laboratory samples, J. metamorphic Geol. 9, 665-670, 1991.

Koehl, J-B. P., Bergh, S. G., Henningsen, T. and Faleide, J. I.: Mid/Late Devonian-Carboniferous collapse basins on the Finnmark Platform and in the southwesternmost Nordkapp basin, SW Barents Sea, Solid Earth, 2018.

Koehl, J-B. P., Bergh, S. G., Osmundsen P-T., Redfield, T. F., Indrevær, K., Lea, H. and Bergø, E.: Late Devonian-Carboniferous faulting in NW Finnmark and controlling fabrics, Norwegian Journal of Geology, submitted.

Krumm, S.: Illitkristallinität als Indikator schwacher Metamorphose – Methodische Untersuchungen, regionale Anwendungen und Vergleiche mit anderen Parametern, Erlanger geol. Abh., 1-75, 1992.

Kübler, B.: La cristallinité de l'illite et les zones tout à fait supérieures du métamorphisme, Colloque sur les „Etages Tectoniques“, 18-21 avril 1966, Festschrift: 105.122; Neuchâtel, 1967.

Kübler, B.: Evaluation quantitative du métamorphisme par la cristallinité de l´illite, Bull. Centre Rech. Pau-S.N.P.A., 2, 385-397, 1968.

Kübler, B.: Les indicateurs des transformations physiques et chimiques dans la diagenèse, température et calorimétrie, in: Thermobarométrie et barométrie géologiques, M. Lagache (ed), Soc. Franc. Minéral. Cristallogr., Paris, 489-596, 1984.

Larssen, G. B., Elvebakk, G., Henriksen, S. E., Nilsson, I., Samuelsberg, T. J., Svånå, T. A., Stemmerik, L. and Worsley D.: Upper Palaeozoic lithostratigraphy of the Southern Norwegian Barents Sea, Norwegian Petroleum Directorate Bulletin, 9, 76 pp., 2002.

Lea, H.: Analysis of Late plaeozoic-Mesozoic brittle faults and fractures in West-Finnmark: geometry, kinematics, fault rocks and the relationship to offshore structures on the Finnmark Platform in the SW Barents Sea, Unpublished Master's Thesis, University of Tromsø, 129 pp., 2016.

Lerman, R.: High temperature fluids and calcite vein formation in the Montana disturbed belt west-central Montana, Unpublished Master's Thesis, University of Montana, 1999.

Li, Z. X., Li, X. H., Kinny, P. D. and Wang, J.: The breakup of Rodinia: did it start with a mantle plume beneath South China?, Earth Planet. Sci. Lett., 173, 171-181, 1999.

Li, Z. X., Bogdanova, S. V., Collins, A. S., Davidson, A., De Waele, B., Ernst, R. E., Fitzsimons, I. C. W., Fuck, R. A., Gladkochub, D. P., Jacobs, J., Karlstrom, K. E., Lu, S., Natapov, L. M., Pease, V., Pisarevsky, S. A., Thrane, K. and Vernikovsky, V.: Assembly, configuration, and break-up history of Rodinia: A synthesis, Precambrian Research, 160, 179-210, 2008.

Lippard, S. J. and Prestvik, T.: Carboniferous dolerite dykes on Magerøy: new age determination and tectonic significance, Norsk Geologisk Tidsskrift, 77, 159-163, 1997.

Lippard, S. J. and Roberts, D.: Fault systems in Caledonian Finnmark and the southern Barents Sea, Nor. geol. unders. bull., 410, 55-64, 1987.

Lovera, O. M., Richter, F. M. and Harrison, T. M.: The $^{40}Ar/^{39}Ar$ Thermochronometry for Slowly Cooled Samples Having a Distribution of Diffusion Domian Sizes, Journal of Geophysical Research, 94, 17917-17935, 1989.

Lyons, J. B. and Snellenburg, L.: Dating faults, Geological Society of America Bulletin, 82, 1749-1752, 1971.

Moore, D. M. and Reynolds, R. C.: X-Ray Diffraction and the Identification and Analysis of Clay Minerals, 2nd edn. Oxford University Press, New York, 1997.

Morley, C. K., von Hagke, C., Hansberry, R., Collins, A., Kanitpanyacharoen, W. and King, R.: Review of major shale-dominated detachment and thrust characteristics in the diagenetic zone: Part II, rock mechanics and microscopic scale, Earth-Science Reviews, 176, 19-50, 2018.

Nasuti, A., Roberts, D. and Gernigon, L.: Multiphase mafic dykes in the Caledonides of northern Finnmark revealed by a new high-resolution aeromagnetic dataset, Norwegian Journal of Geology, 95, 251-263, 2015.

Nieto, F., Pilar Mata, M., Bauluz, B., Giorgetti, G., Árkai, P. and Peacor, D. R.: Retrograde diagenesis, a widespread process on a regional scale, Clay Minerals, 40, 93-104, 2005.

Nystuen, J. P., Andresen, A., Kumpulainen, R. A. and Siedlecka, A.: Neoproterozoic basin evolution in Fennoscandia, East Greenland and Svalbard, Episodes, 31, 35-43, 2008.

Olesen, O., Bering, D., Brönner, M., Dalsegg, E., Fabian, K., Fredin, O., gellein, J., Husteli, B., Magnus, C., Rønning, J. S., Solbakk, T., Tønnesen J. F. and Øverland, J. A.: Tropical Weathering In Norway, TWIN Final Report, Geological Survey of Norway, 188, 2012.

Olesen, O., Kierulf, H. P., Brönner, M., Dalsegg, E., Fredin, O. and Solbakk, T.: Deep weathering, neotectonics and strandflat formation in Nordland, northern Norway, Norwegian Journal of Geology, 93, 189-213, 2013.

Passe, C. R.: The structural geology of east Snøfjord, Finnmark, North Norway, Unpublished Ph.D. Thesis, University of Wales, 1978

Pastore, Z., Fichler, C. and McEnroe, S. A.: The deep crustal structure of the mafic-ultramafic Seiland Igneous Province of Norway from 3-D gravity modelling and geological implications, Geophys. J. Int., 207, 1653-1666, 2016.

Pharaoh, T. C., Macintyre, R. M. and Ramsay, D. M.: K-Ar age determinations on the Raipas suite in the Komagfjord Window, northern Norway, Norsk Geologisk Tidsskrift, 62, 51-57, 1982.

Pharaoh, T. C., Ramsay, D. M. and Jansen, Ø.: Stratigraphy and Structure of the Northern Part of the Repparfjord-Komagfjord Window, Finnmark, Northern Norway, Nor. geol. unders., 377, 1-45, 1983.

Ramberg, I. B., Bryhni, I., Nøttvedt, A. and Rangnes , K.: The making of a land. Geology of Norway, The Norwegian geological Association, Oslo, 2008.

Ramsay, M., Sturt, B. A. and Andersen, T. B.: The sub-Caledonian Unconformity on Hjelmsøy – New Evidence of Primary Basement/Cover Relations in the Finnmarkian Nappe Sequence, Nor. geol. unders., 351, 1-12, 1979.

Ramsay, D. M., Sturt, B. A., Jansen, Ø, Andersen, T. B. and Sinha-Roy, S.: The tectonostratigraphy of western Porsangerhalvøya Finnmark, north Norway, in The Caledonides Orogen – Scandinavia and Related Areas, eds. D. G. Gee and B. A. Sturt, John Wiley & Sons Ltd, 1985.

Reitan, P. H.: The geology of the Komagfjord tectonic window of the Raipas suite Finmark, Norway, Nor. geol. unders., 221, 74, 1963.

Roberts, D.: Patterns of folding and fracturing in North-east Sørøy, Nor. geol. unders., 269, 89-95, 1971.

Roberts, D.: geologisk kart over Norge, berggrunnskart. Hammerfest 1:250 000, Nor. geol. unders., 1973.

Roberts, D. and Lippard, S. J.: Inferred Mesozoic faulting in Finnmark: current status and offshore links, Nor. geol. unders. bull., 443, 55-60, 2005.

Roberts, D., Mitchell, J. G. and Andersen, T. B.: A post-Caledonian dyke from Magerøy North Norway: age and geochemistry, Norwegian Journal of Geology, 71, 289-294, 1991.

Roberts, D., Chand, S. and Rise, L.: A half-graben of inferred Late Palaeozoic age in outer Varangerfjorden, Finnmark: evidence from seismic reflection profiles and multibeam bathymetry, Norwegian Journal of Geology, 91, 191-200, 2011.

Samuelsberg, T. J., Elvebakk, G. and Stemmrik, L.: Late Paleozoic evolution of the Finnmark Platform, southern Norwegian Barents Sea, Norwegian Journal of Geology, 83, 351-362, 2003.

Schaller, M., von Blanckenburg, F., Veldkamp, A., Tebbens, L. A., Hovius, N. and Kubik, P. W.: a 30 000 yr record of erosion rates from cosmogenic 10Be in Middle European river terraces, Earth Planet. Sci. Lett., 204, 307-320, 2002.

Scholz, C. H.: The brittle-plastic transition and the depth of seismic faulting, Geologische Rundschau, 77/1, 319-328, 1988.

Schumacher, E.: Herstellung von 99,9997% ^{38}Ar für die ^{40}K/^{40}Ar Geochronologie, Geochron. Chimia, 24, 441-442, 1975.

Siedlecka, A. and Siedlecki, S.: Some new aspects of the geology of Varanger peninsula (Northern Norway), Nor. geol. unders., 247, 288-306, 1967.

Siedlecka, A., Roberts, D., Nystuen, J. P. and Olovyanishnikov, V. G.: Northeastern and northwestern margins of Baltica in Neoproterozoic time: evidence from the Timanian and Caledonian Orogens, in Gee, D. G. and Pease, V. (eds) 2004, The Neoproterozoic Timanide Orogen of Eastern Baltica, Geological Society, London, Memoirs, 30, 169-190, 2004.

Siedlecki, S.: Geologisk kart over Norge, berggrunnskart Vadsø – M 1:250 000. Nor. geol. unders., 1980.

Steiger, R. H. and Jäger, E.: Subcommission on Geochronology: Convention on the Use of Decay Constants in Geo- and Cosmochronology, Earth Planet. Sci. Lett., 36, 359-362, 1977.

Steltenpohl, M. G., Moecher, D., Andresen, A., Ball, J., Mager, S. and Hames, W. E.: The Eidsfjord shear zone, Lofoten-Vesterålen, north Norway: An Early Devonian, paleoseismogenic low-angle normal fault, Journal of Structural Geology, 33, 1023-1043, 2011.

Stemmerik, L.: Late Palaeozoic evolution of the North Atlantic margin of Pangea, Palaeogeography, Palaeoclimatology, Palaeoecology, 161, 95-126, 2000.

Thyberg, B. and Jahren, J.: Quartz cementation in mudstones: sheet-like quartz cement from clay mineral reactions during burial, Petroleum Geoscience, 17, 53-63, 2011.

Thyberg, B., Jahren, J., Winje, T., Bjørlykke, K., Faleide, J. I. and Marcussen, Ø.: Quartz cementation in Late Cretaceous mudstones, northern North Sea: Changes in rock properties due to dissolution of smectite and precipitation of micro-quartz crystals, Marine and Petroleum Geology, 27, 1752-1764, 2010.

Torgersen E., G. Viola, H. Zwingmann and C. Harris. 2014. Structural and temporal evolution of a reactivated brittle-ductile fault – Part II: Timing of fault initiation and reactivation by K-Ar dating of synkinematic illite/muscovite. Earth Planet. Sci. Lett., vol. 407, pp. 221-233.

Torgersen, E., Viola, G., Zwingmann, H. and Henderson, I. H. C.: Inclined K-Ar illite age spectra in brittle fault gouges: effects of fault reactivation and wall-rock contamination, Terra Nova, 27, 106-113, 2015.

Torsvik, T. H. and Rehnström, E. M.: Cambrian palaeomagnetic data from Baltica: implications for true polar wander and Cambrian palaeogeography, Journal of the Geological Society, 158, 321-329, 2001.

Townsend, C.: Thrust transport directions and thrust sheet restoration in the Caledonides of Finnmark, North Norway, Journal of Structural Geology, 9, 345-352, 1987a.

Townsend, C.: The inner shelf of North Cape, Norway and its implications for the Barents Shelf-Finnmark Caledonide boundary, Norsk Geologisk Tidsskrift, 67, 151-153, 1987b.

Triana R., J. M., Herrera R., J. F., Ríos R., C. A., Castellanos A., O. M., Henao M., J. A., Williams, C. D. and Roberts, C. L.: Natural zeolites filling amygdales and veins in basalts from the British Tertiary Igneous Province on the Isle of Skye, Scotland, Earth Sci. Res. J., 16, 41-53, 2012.

Velde, B.: Experimental determination of muscovite polymorph stabilities, The American Mineralogist, 50, 436-449, 1965.

Vetti, V. V.: Structural development of the Håsteinen Devonian Massif, its Caledonian substrate and the subjacent Nordfjord-Sogn Detachment Zone – a contribution to the understanding of Caledonian contraction and Devonian extension in West Norway, Unpublished Ph.D. Thesis, University of Bergen, 481, 2008.

Viola, G., Zwingmann, H., Mattila, J. and Käpyaho, A.: K-Ar illite age constraints on the Proterozoic formation and reactivation history of a brittle fault in Fennoscandia, Terra Nova, 25, 236-244, 2013.

Vrolijk, P. and van der Pluijm, B. A.: Clay gouge, Journal of Structural Geology, 21, 1039-1048, 1999.

Warr, L. N. and Cox, S.: Clay mineral transformations and weakening mechanisms along the Alpine Fault, New Zealand, in: Holdsworth, R.E., Strachan, R. A., Magloughlin, J. F. and Knipe, R. J. (eds) 2001, The Nature and Tectonic Significance of Fault Zone Weakening, Geological Society, London, Special Publications, 186, 85-101, 2001.

Wemmer, K.: K/Ar-Altersdatierungsmöglichkeiten für retrograde Deformationsprozesse im spröden und duktilen Bereich - Beispiele aus der KTB-Vorbohrung (Oberpfalz) und dem Bereich der Insubrischen Linie (N-Italien), Göttinger Arb. Geol. Paläont., 51, 1-61, 1991.

Whitney, G. and Northrop, H. R.: Experimental investigation of the smectite to illite reacton: Dual reaction mechanisms and oxygen-isotope systematics, American Mineralogist, 73, 77-90, 1988.

Worley, W. G. and Tester, J. W.: Dissolution of Quartz and Granite in Acidic and Basic Salt Solutions, in Worldwide Utilization of Geothermal Energy: an Indigenous, Environmentally Benign Renew-able Energy Resource, proceedings of the World geothermal Congress (May 18-31, 1995: Florence Italy), International Geothermal Association, Inc., Auckland, New-Zealand, 4, 2545-2551, 1995.

Worthing, M. A.: Fracture patterns on Eastern Seiland, North Norway and their possible Relationship to Regional Faulting, Nor. geol. unders. bull., 398, 35-41, 1984.

Zwaan, K. B.: Geology of the West Troms Basement Complex, northern Norway, with emphasis on the Senja Shear Belt: a preliminary account, Nor. geol. unders. bull., 427, 33-36, 1995.

Zwaan, K. B. and Gautier, A. M.: Alta and Gargia. Description of the geological maps (AMS-M711) 1834 1 and 1934 IV 1:50 000, Nor. geol. unders., 357, 1-47, 1980.

Zwaan, K. B. & Roberts, D.: Tectonostratigraphic Succession and Development of the Finnmarkian Nappe Sequence, North Norway, Nor. geol. unders., 343, 53-71, 1978.

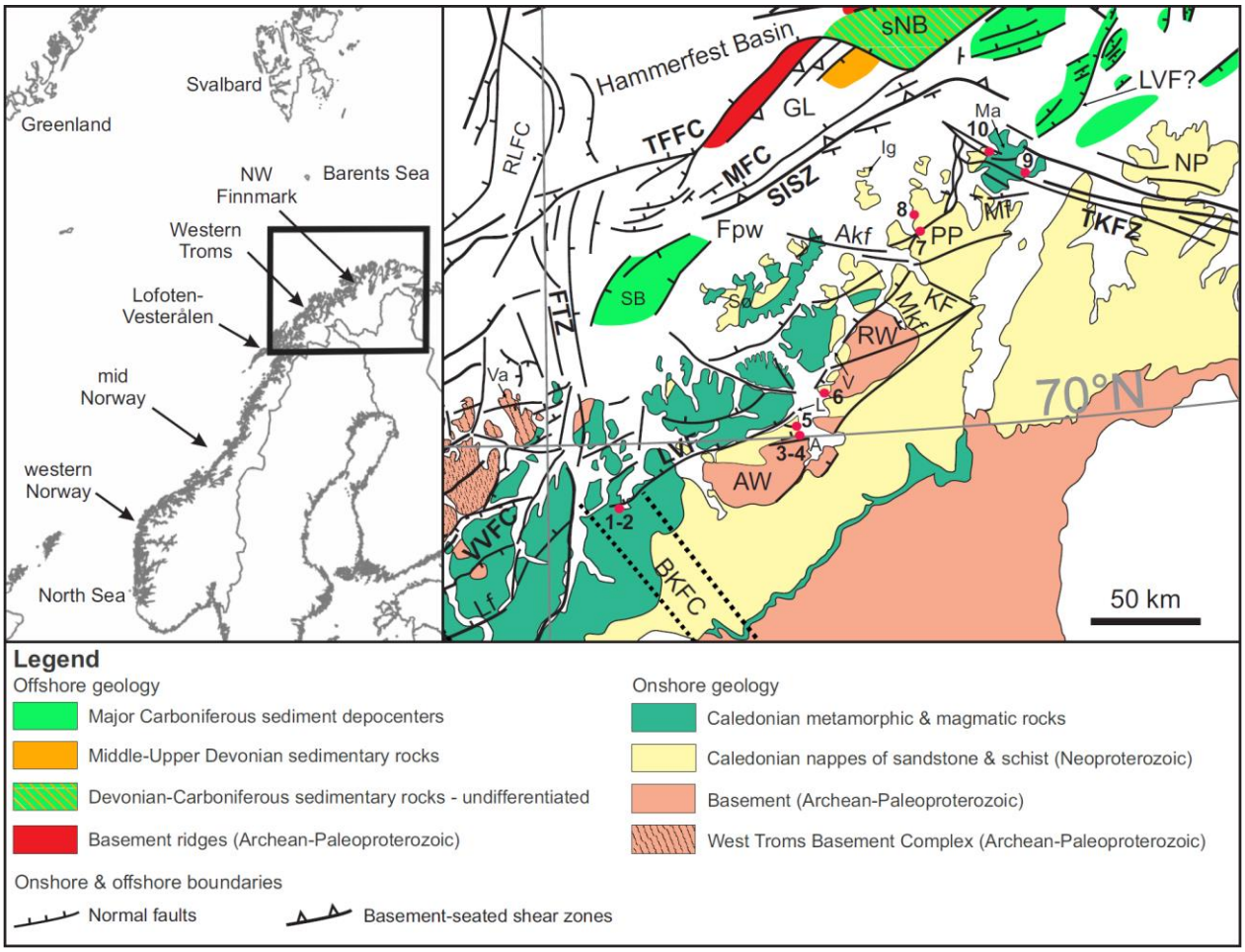

Figure 1: The upper left inset shows the location of the study area (NW Finnmark) along the Norwegian continental shelf as a black frame. The upper right inset shows a tectonic map of NW Finnmark showing the location of dated brittle faults as red dots numbered as follows: (1) = Sørkjosen 1; (2) = Sørkjosen 2; (3) = Altafjorden 1; (4) = Altafjorden 2; (5) = Talvik; (6) = Storekorsnes; (7) = Snøfjorden-Slatten; (8) = Porsanger; (9) = Honningsvåg; (10) = Gjesvær. Map modified after Indrevær et al., (2013) and Koehl et al. (2018). Abbreviations: A = Altafjorden; Akf =Akkarfjord fault; AW = Alta-Kvænangen tectonic window; BKFC = Bothnian-Kvænangen Fault Complex; FPw = Finnmark Platform west; FTZ = Fugløya transfer zone; GL = Gjesvær Low; Ig = Ingøya; KF = Kokelv Fault; L = Langfjorden; LVF = Langfjord-Vargsund fault; Ma = Magerøya; Mf = Magerøysundet fault; MFC = Måsøy Fault Complex; Mkf = Markopp fault; NP = Nordkinn Peninsula; PP = Porsanger Peninsula; RLFC = Ringvassøya-Loppa Fault Complex; RW = Repparfjord-Komagfjord tectonic window; SB = Sørvær Basin; SISZ = Sørøya-Ingøya shear zone; sNB = southwesternmost Nordkapp basin; Sø = Sørøya; TFFC = Troms-Finnmark Fault Complex; TKFZ = Trollfjorden-Komagelva Fault Zone; V = Vargsundet; Va = Vanna; VVFC = Vestfjorden-Vanna fault complex.

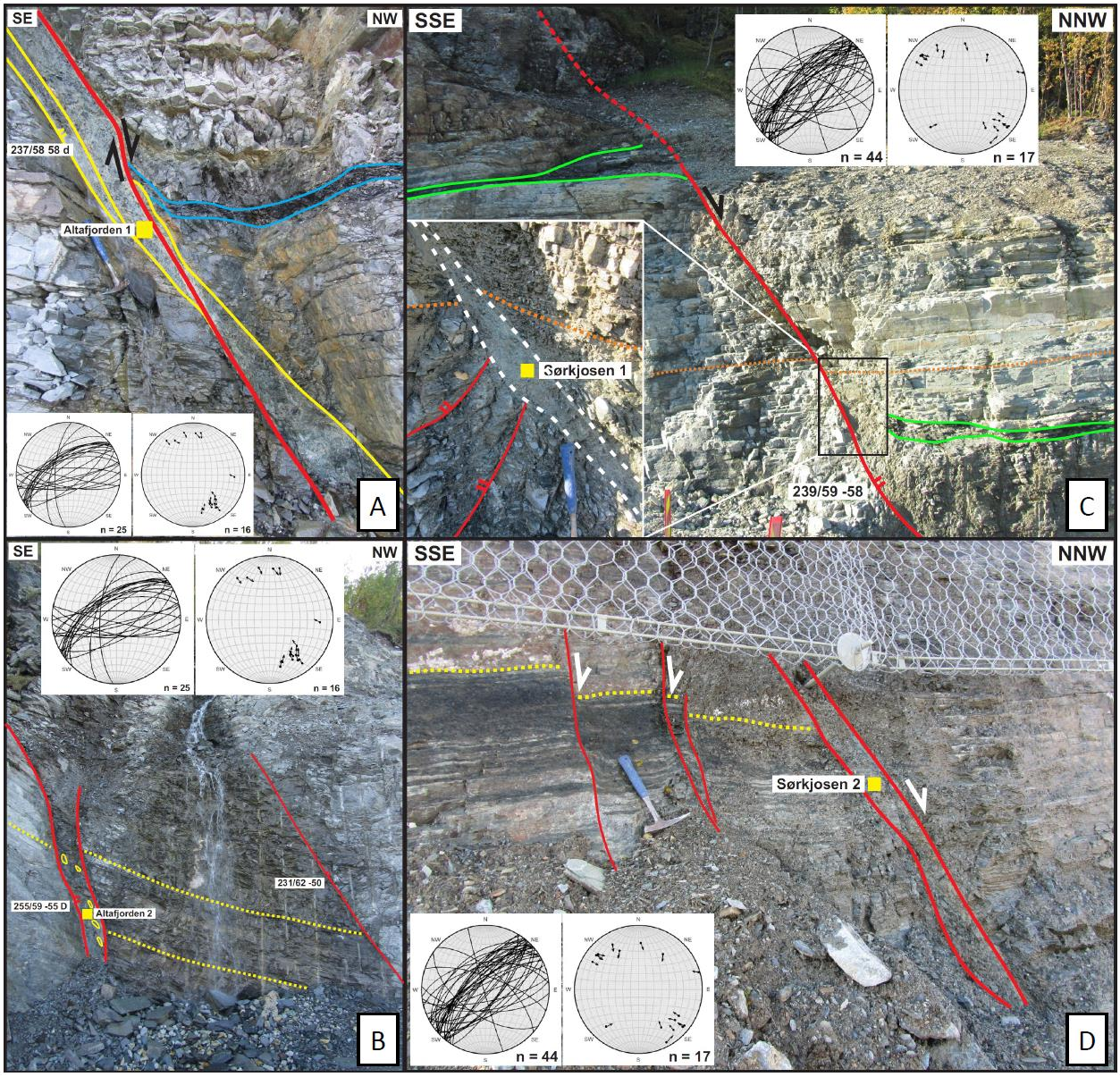
SE
NW
237/58 58 d
Altafjorden 1
n = 25
n = 16
A
SSE
NNW
n = 44
n = 17
Sørkjosen 1
239/59 -58
C
SE
NW
n = 25
n = 16
231/62 -50
255/59 -55 D
Altafjorden 2
B
SSE
NNW
Sørkjosen 2
n = 44
n = 17
D

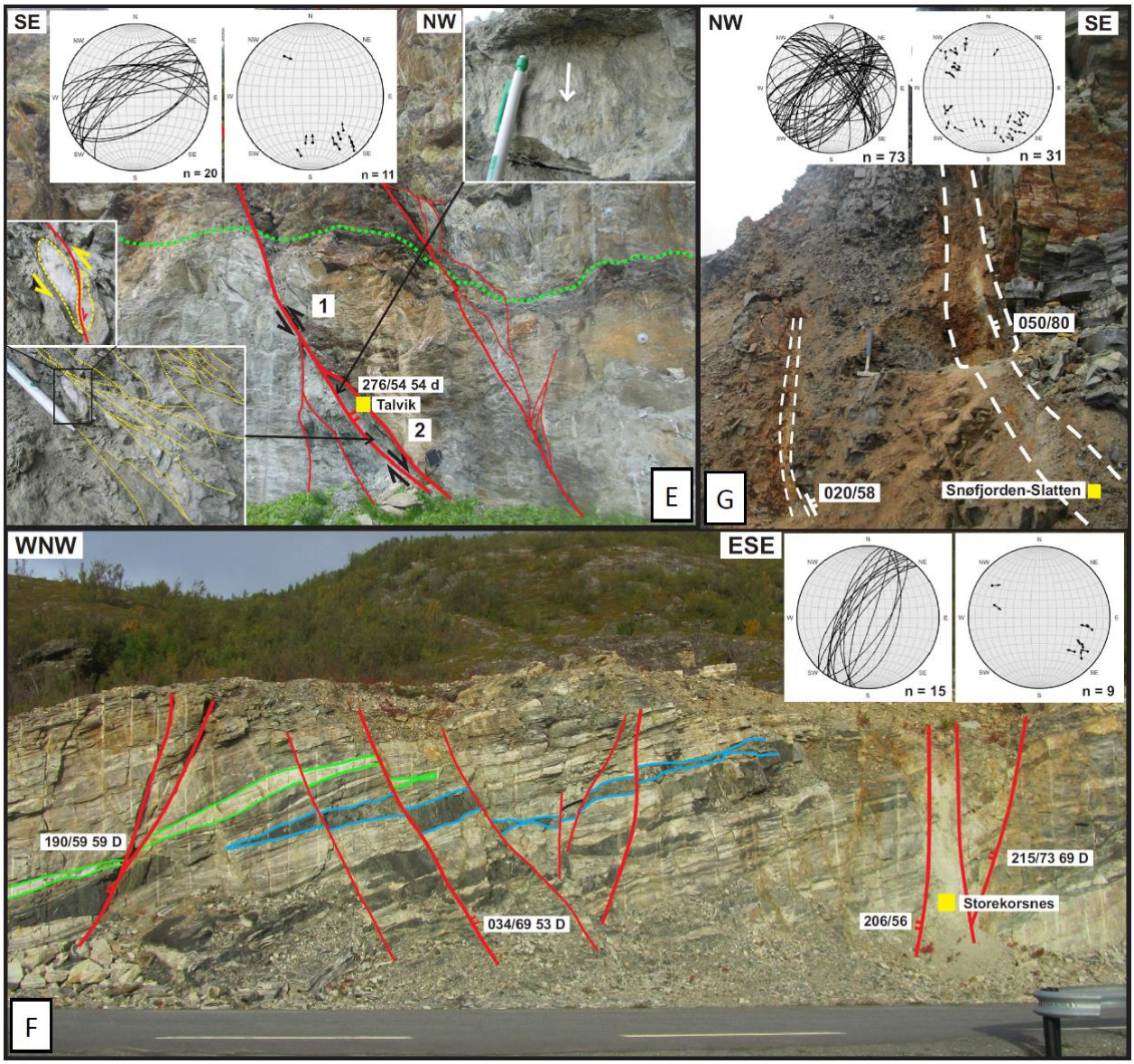
SE
NW
n = 20
n = 11
1
276/54 54 d
Talvik
2
E
NW
SE
n = 73
n = 31
050/80
020/58
Snøfjorden-Slatten
G
WNW
ESE
n = 15
n = 9
190/59 59 D
034/69 53 D
215/73 69 D
Storekorsnes
206/56
F

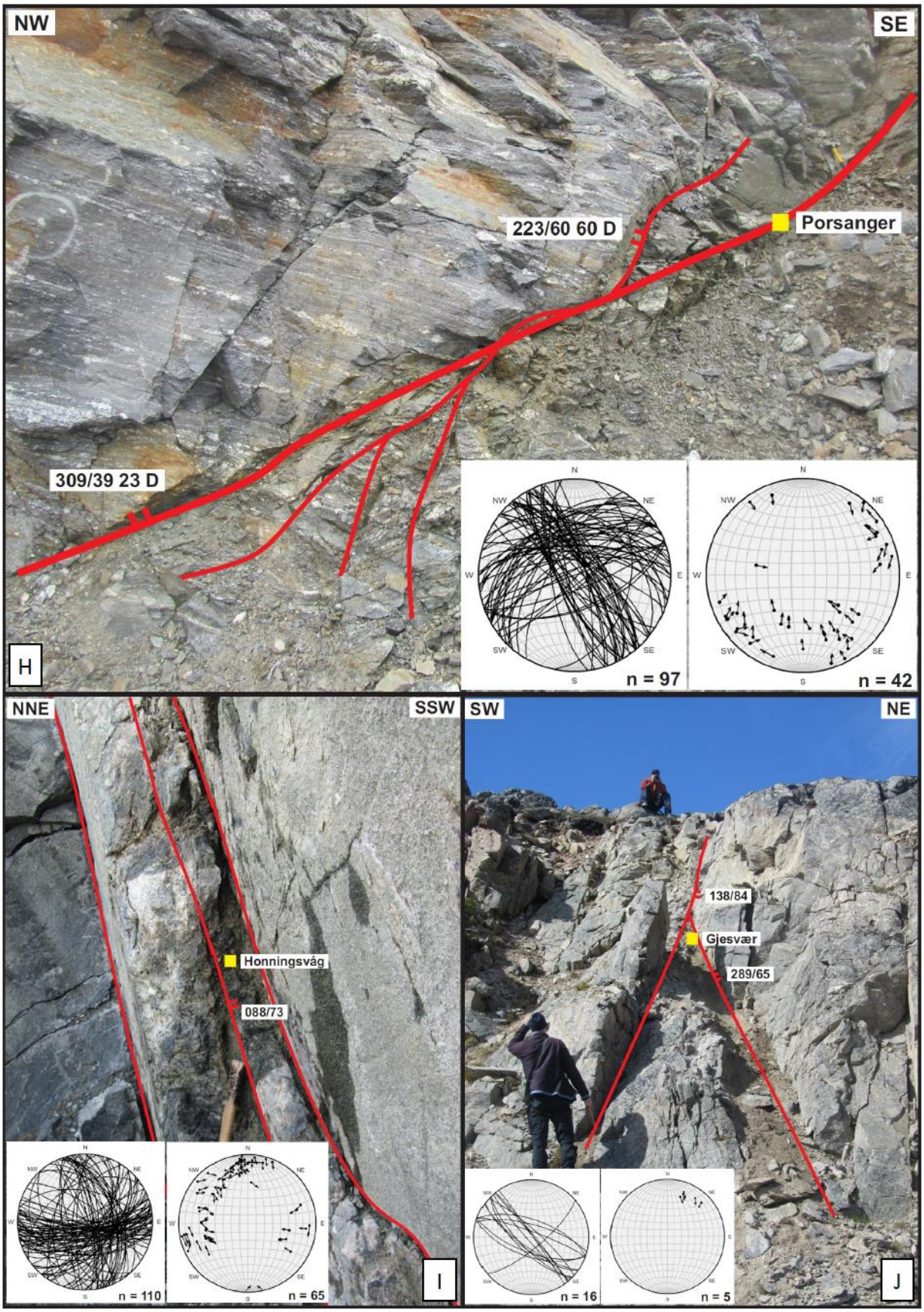

Figure 2: Outcrop photographs of the dated faults. Each photograph is accompanied of the location of the dated samples (yellow squares), structural measurements presented in white boxes and in Schmidt stereonets (left hand-side stereonets show fracture surfaces as great circles and right hand-side stereonets

display slickenside lineations as pole to fault surfaces indicating the movement of the hanging-wall), and potential kinematic indicators where available. (a) ENE-WSW trending, NW-dipping Altafjorden fault 1 (sample 3) crosscutting Precambrian rocks of the Alta-Kvænangen tectonic window along the western shore of Altafjorden. A potentially drag-folded mafic bed is shown in blue. Modified after Koehl et al (submitted); (b) ENE-WSW trending, NW-dipping Altafjorden fault 2 (sample 4) within the Alta-Kvænangen tectonic window. The country-rock displays preserved bedding surfaces (in dotted yellow); (c) ENE-WSW trending, NW-dipping fault in the footwall of the Sørkjosen fault (Sørkjosen 1; sample 1). A potentially offset mafic bed is shown in green and the bedrock fabric in dotted orange. The lower left frame is a zoom in the fault-core displaying the location of the dated sample; (d) ENE-WSW trending, NW-dipping fault in the footwall of the Sørkjosen fault (Sørkjosen 2; sample 2). Dotted yellow lines show normal offsets of mafic beds across brittle faults; (e) E-W trending, N-dipping Talvik fault (sample 5) crosscutting rocks of the Kalak Nappe Complex along the western shore of Altafjorden. Kinematic indicators include ductile fabrics made of microshears (lower left frame), sigma-clasts (middle left frame) and slickenside lineations (upper right frame). The bedrock fabric is shown in green. Modified after Koehl et al (submitted); (f) NNE-SSW trending brittle faults crosscutting rocks of the Kalak Nappe Complex along the eastern shore of Altafjorden (sample 6). See normal offsets of geological markers (in green and blue). Modified after Koehl et al (submitted); (g) NE-SW trending, SE-dipping fault segment of the Snøfjorden-Slatten fault (sample 7) in Snøfjorden, on the Porsanger Peninsula. Modified after Koehl et al (submitted); (h) Low-angle, WNW-ESE trending, NE-dipping fault (sample 8) crosscutting rocks of the Kalak Nappe Complex on the Porsanger Peninsula; (i) Steep, E-W to WNW-ESE trending faults (sample 9) within the gabbroic rocks of the Honningsvåg Igneous Complex; (j) Steep, WNW-ESE trending brittle faults near Gjesvær (sample 10), in the western part of Magerøya. The faults crosscus rocks of the Kalak Nappe Complex.

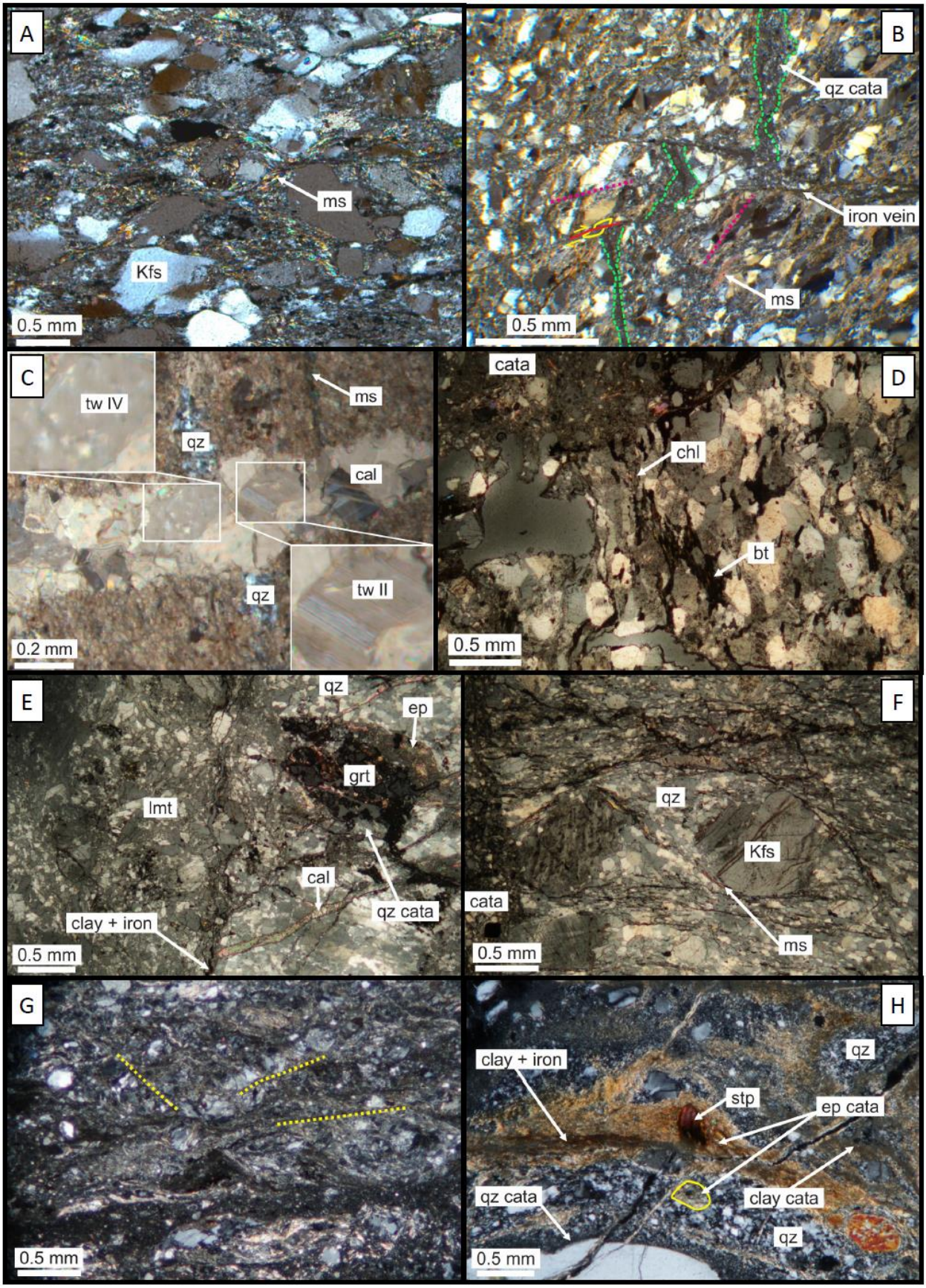
A
ms
Kfs
0.5 mm
B
qz cata
iron vein
ms
0.5 mm
C
tw IV
ms
qz
cal
qz
tw II
0.2 mm
cata
D
chl
bt
0.5 mm
E
qz
ep
grt
lmt
cal
qz cata
clay + iron
0.5 mm
F
qz
Kfs
cata
ms
0.5 mm
G
0.5 mm
H
clay + iron
qz
stp
ep cata
qz cata
clay cata
qz
0.5 mm

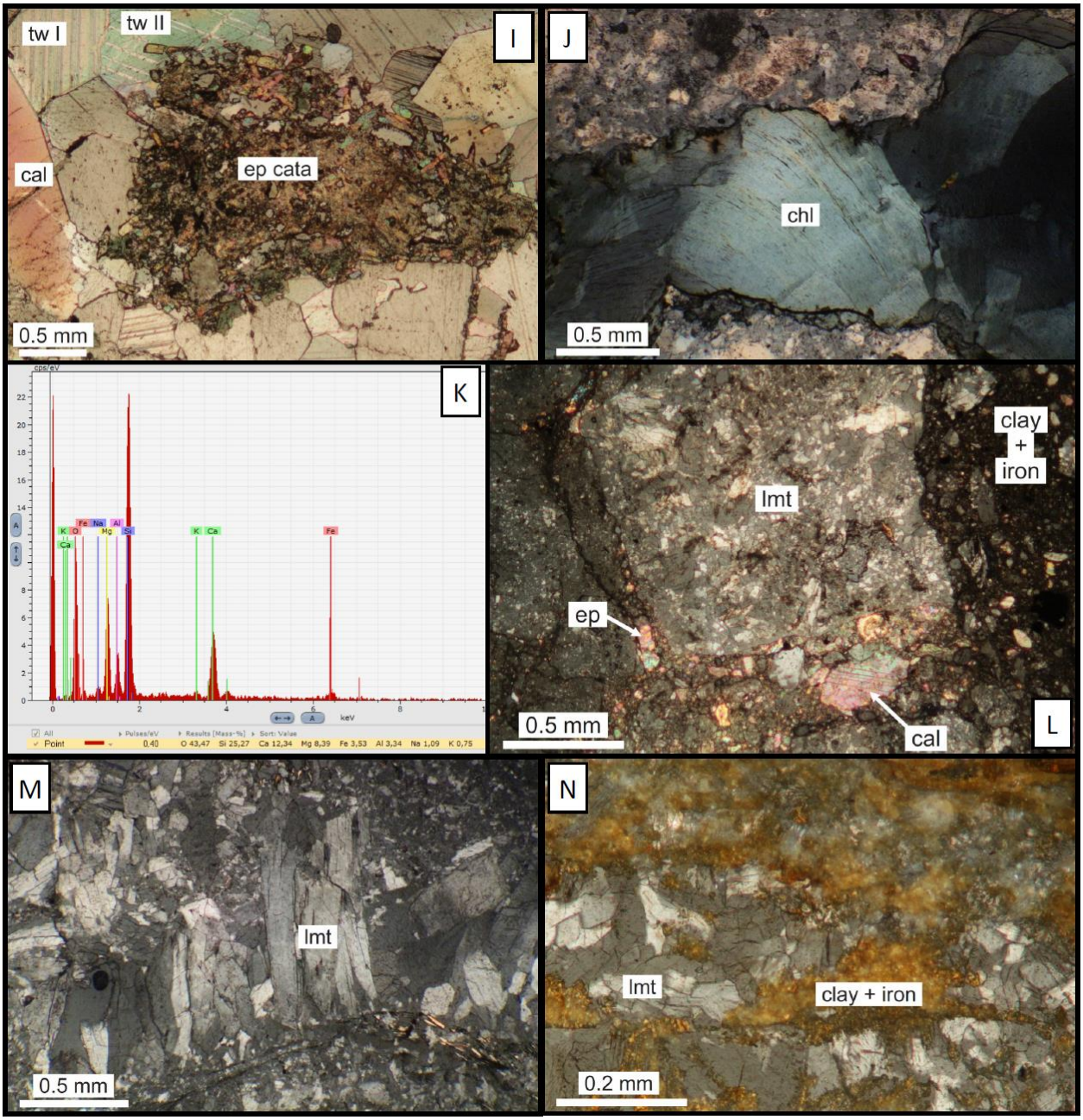

Figure 3: Microscope photographs of cataclasite and hostrock in NW Finnmark. (a) Precambrian S-C foliation made of muscovite (ms) microcrystals surrounding K-feldspar (Kfs) sigma-clasts; (b) Cataclasite vein (dashed green) in Precambrian basement rocks seemingly offset by iron- and clay-rich fractures that formed parallel to existing S-C foliation deformation planes (dotted pink). The amount of offset across iron-rich fractures is shown by a dextrally (red) offset, sheared quartz grain (yellow) and is lower than the apparent offset of the cataclastic vein in green; (c) Calcite-filled (cal) fracturein Precambrian basement rocks crosscutting a vein of recrystallized quartz (qz) and a muscovite-bearing (ms) ductile microshear. Calcite cement crystals typically show type II (tw II; lower right inset) and type IV (tw IV; upper left inset) twinnings; (d) Preserved biotite (bt) foliation in Caledonian host rocks near a cataclastic (cata) brittle fault. Approaching the fault, biotite is increasingly recrystallized into chlorite (chl); (e) Highly fractured garnet crystal (grt) in Caledonian host rock crosscut by epidote- (ep; type 1) and quartz-rich cataclasites (qz cata; type 2), which are both truncated by calcite-filled veins (cal; type 3). Both cataclasites and calcite veins are truncated by a third cataclasite made up with a matrix of angular, poorly sorted clasts of laumontite (lmt; type 4) crosscut by late clay and iron-bearing veins (type 5); (f) Caledonian S-C foliation made of muscovite (ms) microcrystals surrounding K-feldspar (Kfs) sigma-clasts that have partly recrystallized into quartz (qz); (g) Cataclastic fault-rock showing the remains of pre-existing S, C and C' foliation deformation planes in dotted yellow along which brittle fractures formed; (h) Epidote-rich cataclasite (ep cata; type 1) in Caledonian host rock including clasts of stilpnomelane (stp) crosscutting quartz-rich host rock (qz) and

truncated by quartz-rich cataclasite (qz cata; type 2), which incorporates clasts of epidte-rich cataclasite (yellow; type 1). Ep- (type 1) and quartz-rich (type 2) cataclasites are truncated by subsequent clay and iron-rich veins (type 5); (i) Epidote-rich cataclasite (ep cata; type 1) embedded within a calcitic cement (cal; type 3) made of large crystals showing type I (tw I) and type II (tw II) twinnings; (j) Fracture with chlorite (chl) precipitation related with type 1 cataclasite; (k) SEM analysis of the atomic composition of the stilpnomelane crystal shown in type 1 cataclasite in (h). The numbers below the graph represent mass percentage of each atom; (l) Large clasts of laumontite-rich (lmt; type 4) cataclasite crosscut at the bottom of the photograph by a cataclastic vein including clasts of epidote (ep; type 1), quartz (type 2), calcite (cal; type 3) and laumontite (type 4), and on the right hand-side by a cataclastic vein containing mostly iron-bearing and clay minerals (type 5). The iron- and clay-rich cataclasite (type 5) truncates all the other types of cataclasites; (m) Laumontite precipitations (lmt; type 4 cataclasite). Crystals are elongated perpendicular to the fracture along which they precipitated; (n) Iron- and clay-rich (type 5) cataclasite crosscutting mildly fractured late growth of laumontite (lmt; type 4).

Table 1: Mineral composition of dated fault gouges. "Presumed traces" are based on inclined spectra (cf. Appendix 1) showing peaks at 27.3-27.4 for K-feldspar, and on the presence of minor illite in smectite, enabling K/Ar dating, e.g. samples 9 and 10. Abbreviations: chl = chlorite; I = illite; kao = kaolinite; Kfs = K-feldspar; lmt = laumontite; Qz = quartz; S = smectite.

Sample	Grainsize	S	I	Qz	Kfs	plagioclase	chl	kao	lmt?
1	<0.2µm	*	O		-		**		
	<2µm	*	O		-		**		
	2-6µm	**	O	*	-		**		
2	<0.2µm	*	O		-		**		
	<2µm	*	O		-		**		
	2-6µm	*	*	O	-		**		
3	<0.2µm	**	*	O			*		
	<2µm	**	*	O			*		
	2-6µm	**	**	*			**		
4	<0.2µm	**	*				O		
	<2µm	**	*				*		
	2-6µm	**	*	O			O		
5	<0.2µm	**	*				*	*	
	<2µm	**	*	O			**	**	
	2-6µm	*	*	O			**	**	
6	<0.2µm	**	*				*		
	<2µm	**	*	O			*		
	2-6µm	**	O	O	-		*	*	
7	<0.2µm	**	O	O					
	<2µm	**	*	O	-				
	2-6µm	**	*	*	O				
8	<0.2µm	**	*				*		
	<2µm	**	**				*		
	2-6µm	**	**	O			*		
9	<0.2µm	**	-						**
	<2µm	**	-		-				**
	2-6µm	**	-						**
10	<0.2µm	**	-	O	-				
	<2µm	**	-	O	-				
	2-6µm	**	-	*	O	O			

** major component * minor component O trace - presumed trace

all smectites are of R=0 type, indicating maximum 10% of Illite content

Table 2: K/Ar ages from synkinematic illite in fault gouge.

Sample	Spike [No.]	K2O [Wt. %]	40 Ar * [nl/g] STP	40 Ar * [%]	Age [Ma]	2s-Error [Ma]	2s-Error [%]
1	5450	0,74	3,85	85,60	**153,4**	1,9	1,2
	5467	1,07	5,52	90,43	**153,2**	3,7	2,4
	5455	1,63	11,52	97,06	**206,8**	2,6	1,3
2	5461	0,70	3,89	43,30	**164,4**	4,5	2,7
	5456	1,00	8,63	99,93	**249,4**	3,3	1,3
	5457	2,29	19,57	96,08	**247,6**	3,7	1,5
3	5431	2,76	92,99	98,78	**824,7**	12,7	1,5
	5437	3,11	102,07	98,46	**806,4**	10,7	1,3
	5430	6,04	277,63	99,55	**1050,7**	12,2	1,2
4	5440	1,01	33,50	94,56	**811,3**	17,8	2,2
	5442	2,77	110,73	98,23	**943,8**	17,3	1,8
	5446	5,58	257,47	99,24	**1054,2**	14,7	1,4
5	5451	1,23	12,14	60,55	**282,1**	6,3	2,2
	5428	1,52	19,11	92,83	**353,7**	4,1	1,2
	5429	1,53	23,84	96,46	**427,3**	8,4	2,0
6	5435	1,34	14,04	65,30	**298,5**	5,0	1,7
	5443	1,63	16,73	73,27	**292,6**	4,0	1,4
	5434	1,25	8,90	67,82	**208,5**	3,1	1,5
7	5438	2,19	14,98	81,40	**200,4**	6,0	2,3
	5454	3,79	29,66	89,43	**227,4**	5,3	3,0
	5449	9,61	78,88	98,61	**238,0**	5,4	2,3
8	5465	3,64	37,86	92,47	**296,6**	3,8	1,3
	5433	3,91	40,80	93,87	**297,6**	7,7	2,6
	5432	5,17	54,91	98,19	**302,3**	6,5	2,2
9	5436	0,12	1,09	23,00	**265,2**	23,6	8,9
	5448	0,19	1,50	26,04	**234,7**	18,0	7,7
	5444	0,37	4,16	47,29	**315,6**	13,6	4,3
10	5441	1,97	18,56	91,27	**270,8**	6,0	2,2
	5445	2,03	20,09	95,44	**284,0**	6,2	2,2
	5447	1,48	16,23	94,71	**312,5**	8,7	2,8

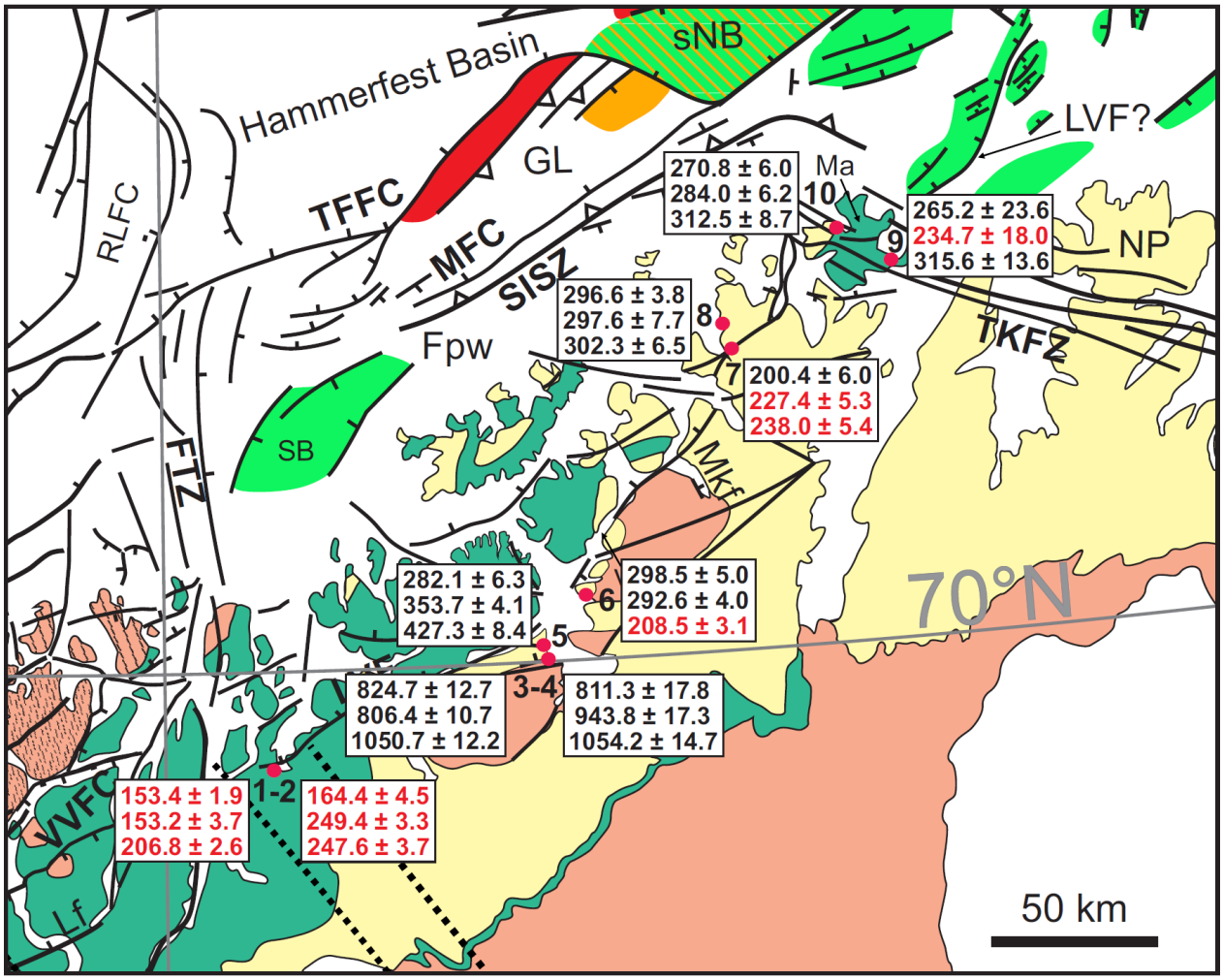

Figure 4: Structural map of the study area showing the obtained K/Ar ages for each sample, including from top to bottom finest, intermediate and coarsest grainsize fractions. Ages in red are considered erroneous (cf. main text). Map modified after Indrevær et al., (2013) and Koehl et al. (2018). Legend and abbreviations as in Figure .

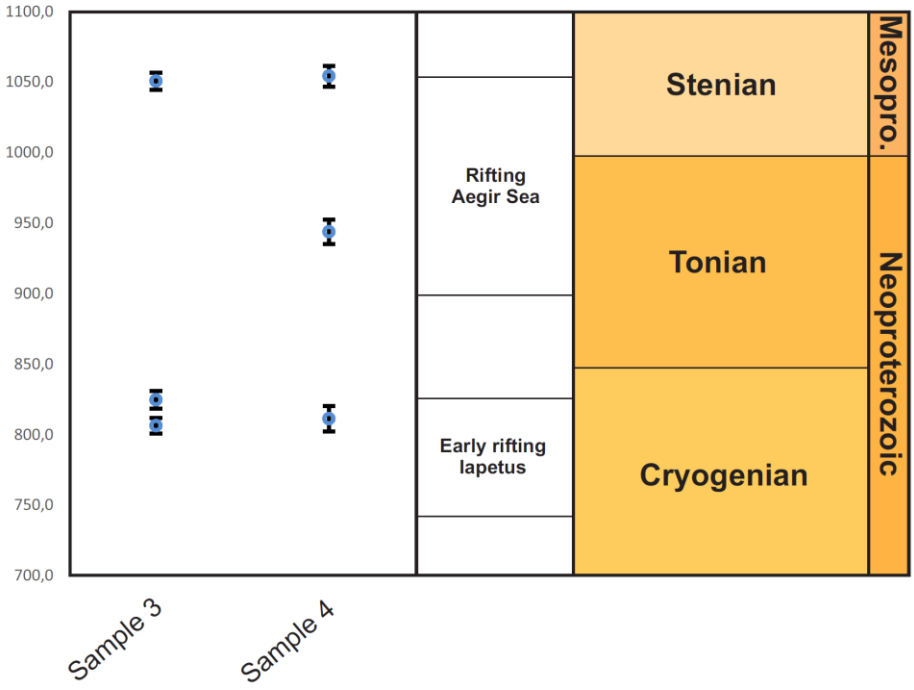

Figure 5: Graph displaying the obtained Precambrian ages for brittle faults in the Alta-Kvænangen tectonic window. The vertical axis is time in Ma and the horizontal axis shows the dated sample numbers, which locations are displayed in Figure & Figure 4. Columns to the right show extensional tectonic events related to the formation of the NW Baltoscandian basins during the opening of the Asgard Sea (Siedlecka et al., 2004; Nystuen et al., 2008; Cawood et al., 2010; Cawood & Pisarevsky, 2017) and to the earliest phase of rifting of the Iapetus Ocean-Ægir Sea (Li et al., 1999, 2008; Torsvik & Rehnström, 2001; Hartz & Torsvik, 2002), and associated geological Periods and Eras.

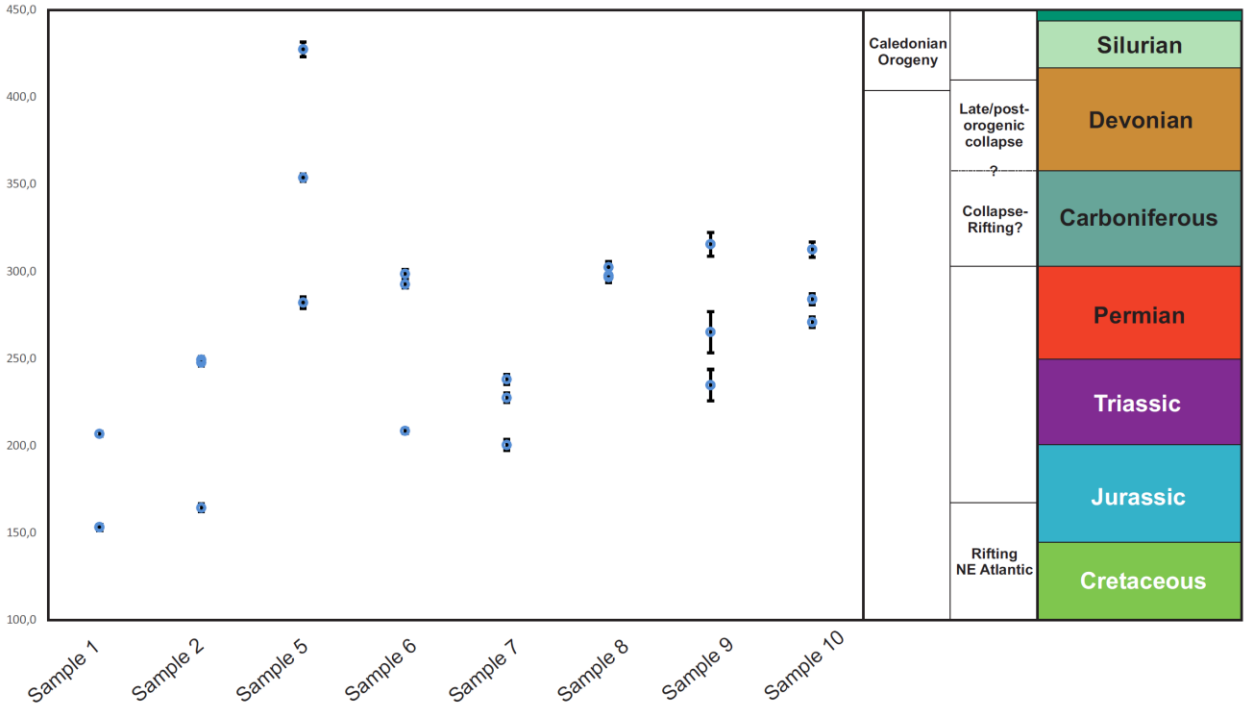

Figure 6: Graph showing the Phanerozoic K/Ar ages and associated error obtained for fault gouge samples in NW Finnmark. The vertical axis represents time in Ma and the horizontal axis shows the dated sample numbers, which locations are displayed in Figure & Figure 4. Columns to the right of the graph display major contractional (based on Ramberg et al., 2008; Vetti, 2008; Corfu et al., 2014) and extensional events (Faleide et al., 1993; Steltenpohl et al., 2011; Koehl et al., 2018) that affected North Norway in late Paleozoic-Mesozoic times, and associated geological time Periods.

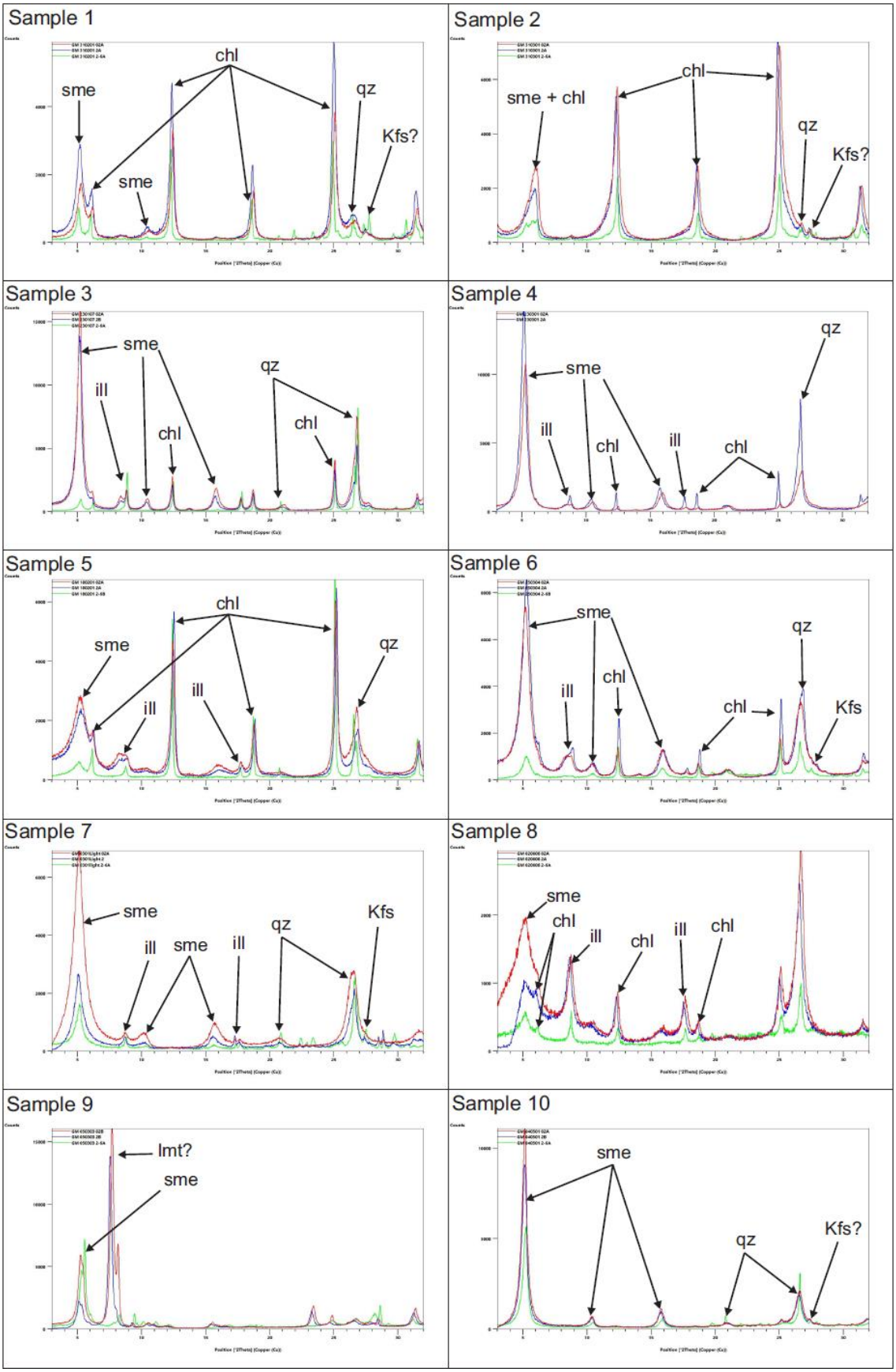

Appendix 1: X-Ray Diffraction spectrum of copper graphs showing the mineralogical composition of the dated fault-rock samples. Green, blue and red lines respectively represent coarse, intermediate and fine grainsize fractions for each sample. Abbreviations: chl = chlorite; ill = illite; Kfs = K-feldspar; lmt = laumontite; qz = quartz; sme = smectite.